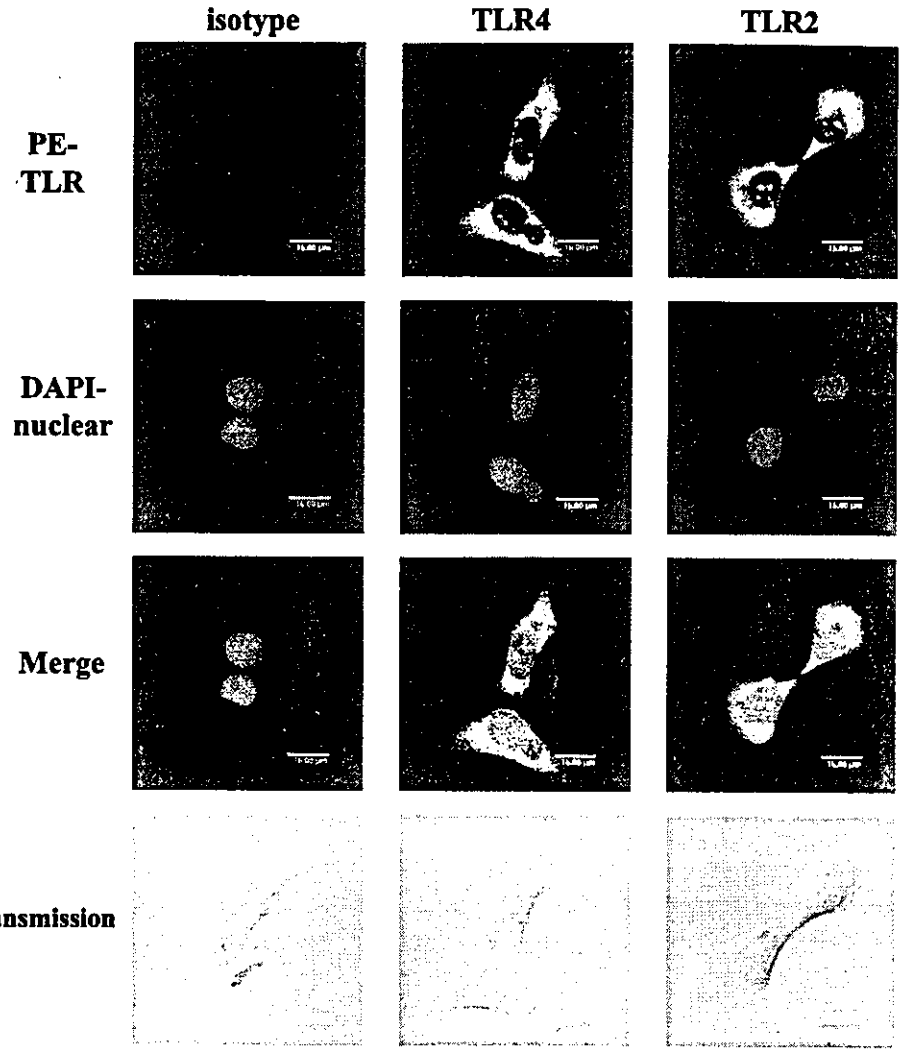

FIGURE 4. Immunohistochemical analysis for the detection of cytoplasmic TLR2 and TLR4 in the human corneal epithelial cell line HCE-T. HCE-T was cultured on a slide chamber, washed with PBS^-, and air-dried. Slides were fixed with methanol for 30 min, then stained with PE-conjugated mouse anti-human TLR2 (TL2.1) or TLR4 (HTA125) mAb or isotype control mouse IgG2a for 24 h at room temperature. Confocal images of HCE-T showed specific staining with anti-TLR2 and -TLR4 mAb in the perinucleic region or cytoplasm. DAPI were used for counterstaining. Each bar represents a length of 50 μm.

Alexa 488-LPS into HCE-T did not lead to the enhancement of NF-κB-mediated signals (Fig. 6*C*). These findings suggest that cytoplasmically expressed TLR4 is not capable of responding to LPS even when the endotoxin is intracellularly introduced.

Discussion

Interestingly, our results indicate that ocular surface epithelial cells, which are an important component of the mucosal immune system, express TLR-specific mRNA for two well-characterized pattern recognition receptors, TLR2 and TLR4. However, incubation with PGN and LPS failed to induce the secretion by HCE-T and primary human corneal epithelial cells of inflammation-associated cytokines such as IL-6 and IL-8. Further, NF-κB activation was not up-regulated by the stimulation of HCE-T with LPS or PGN. These results show that human corneal epithelial cells are incapable of responding to LPS from *P. aeruginosa* and to PGN from *S. aureus*. To support the finding, we subsequently used FACS and immunohistochemical analyses to show that human corneal epithelial cells express TLR2 and TLR4 intracellularly, but not at the cell surface. Even when LPS was artificially delivered to intracellularly expressed TLR4 in the cytoplasm, it did not lead to the subsequent activation of NF-κB-mediated signaling for the induction of IL-6 and IL-8. These findings suggest the interesting possibility that the ocular surface epithelial cell-associated mucosal immune system may create an immunosilent condition for TLR-mediated innate immunity to prevent unnecessary inflammatory responses to normal bacterial flora. However, it has been shown that Langerhans cells and macrophages are located at the basal layer of the corneal epithelium and corneal stroma (33). Thus, these APCs may immediately respond to microbial products via TLRs.

Epithelial cells have long been thought to protect the integrity of mucosal surfaces mainly by acting as a physical barrier to invading pathogens. In fact, the mucosal epithelium serves as a critical immunological barrier against invasion by bacteria and viruses. As well as constituting a physical barrier, mucosal epithelial cells are

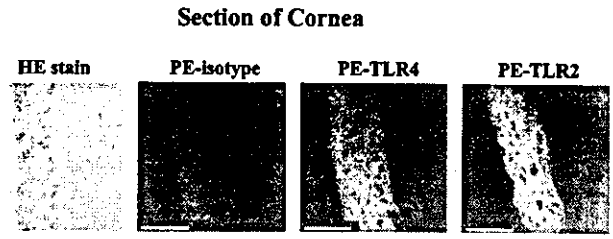

FIGURE 5. Immunohistochemical analysis for the detection of cytoplasmic TLR2 and TLR4 in human corneal epithelium. Slides of tissue sections were fixed with methanol for 30 min and then stained with PE-conjugated mouse anti-human TLR2 (TL2.1) or TLR4 (HTA125) mAbs or isotype control mouse IgG2a for 24 h at room temperature. Tissue sections of human cornea showed specific staining with anti-TLR2 and -TLR4 mAb in the cytoplasm. Each bar represents a length of 50 μm.

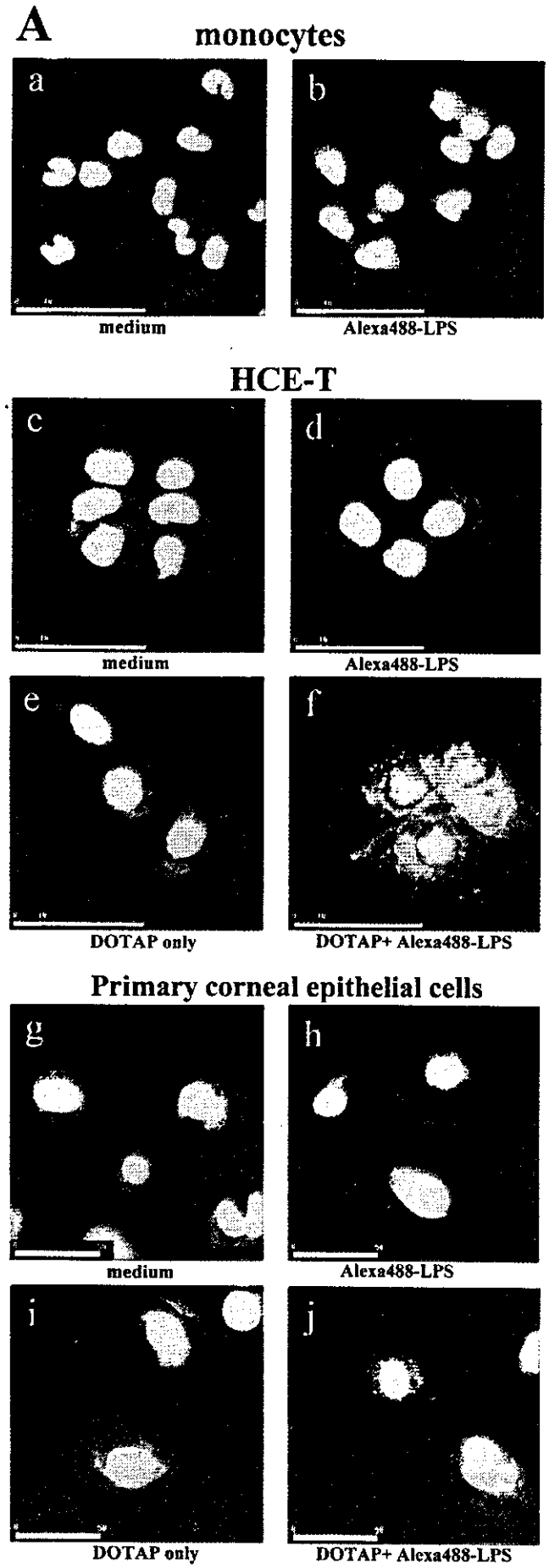
A
monocytes
a
b
medium
Alexa488-LPS
HCE-T
c
d
medium
Alexa488-LPS
e
f
DOTAP only
DOTAP+ Alexa488-LPS
Primary corneal epithelial cells
g
h
medium
Alexa488-LPS
i
j
DOTAP only
DOTAP+ Alexa488-LPS

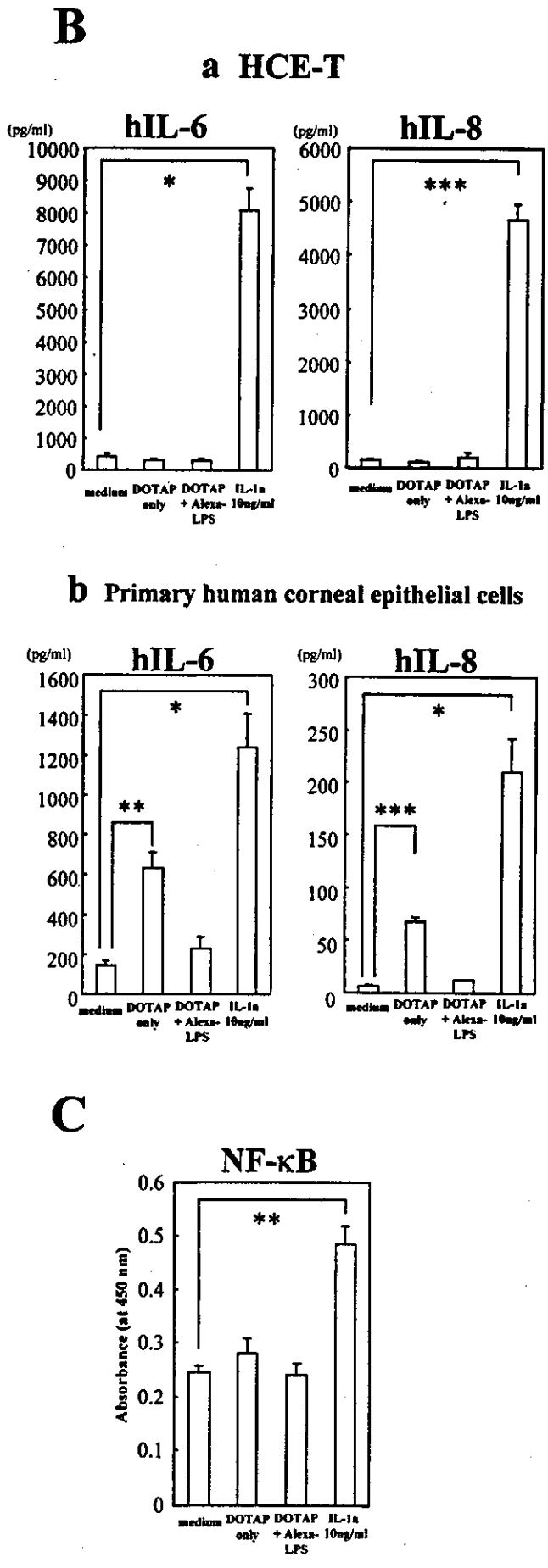
B
a HCE-T
hIL-6
(pg/ml)
10000
9000
8000
7000
6000
5000
4000
3000
2000
1000
0
*
medium
DOTAP only
DOTAP + Alexa-LPS
IL-1a 10ng/ml
hIL-8
(pg/ml)
6000
5000
4000
3000
2000
1000
0
***
b Primary human corneal epithelial cells
hIL-6
(pg/ml)
1600
1400
1200
1000
800
600
400
200
0
*
**
hIL-8
(pg/ml)
300
250
200
150
100
50
0
*
***
C
NF-κB
Absorbance (at 450 nm)
0.6
0.5
0.4
0.3
0.2
0.1
0
**

active participants in innate and acquired mucosal immune responses. When invaded by respiratory or intestinal pathogens, mucosal epithelial cells elicit proinflammatory gene expression, secretion of cytokines and chemokines, and recruitment of inflammatory cells to the site of infection (34). These findings suggest that epithelial cells play a major role in innate immune responses, which probably evolved to limit the infection by pathogenic bacteria at the invasion site. Alternatively, epithelial cells may initiate a sequence of innate and acquired immunity phases for the induction of Ag-specific immunity in both mucosal and systemic compartments. It is thus logical to assume that epithelial cells residing at the mucosal surface continuously express an array of TLR family members as sensors to detect and recognize invading pathogens. To this end, it has been shown that several TLRs, including TLR2 and TLR4, are expressed in the mucosal epithelium of the human trachebronchia (18). After exposure to LPS, human trachebronchial epithelial cells were activated for the expression of increased hBD2 mRNA. Bladder epithelial cells have also been reported to express TLR4 as well as increased levels of proinflammatory cytokines after incubation with LPS (20). In total contrast to these previous results, our findings suggest that the corneal epithelia do not express TLR2 and TLR4 at their cell surface.

To understand these seemingly conflicting findings, one must revisit the immunological and microbiological conditions prevailing in the mucosal epithelium. Even in the absence of pathogens, the mucosal epithelium is continuously exposed to great numbers of commensal bacteria, both Gram-positive and -negative (35, 36). Despite the high density of these commensal bacteria and their biologically active products observed under these physiological circumstances, the mucosal epithelium generally does not activate proinflammatory signaling cascades against them. These commensal bacteria are generally regarded as beneficial microflora for the host because they can suppress pathogens by displacing them from a microbial niche or by secreting antimicrobial substances (36). Normal bacterial flora residing in the conjunctival sac or along the eyelid edge making contact with the corneal surface include coagulase negative staphylococci, *P. acnes,* and others (4, 5). Commensal flora are also key to creating a symbiotic host-parasite interaction for the intestinal mucosa, especially in the large intestine. It is our contention that corneal epithelial cells purposely do not express TLRs (e.g., TLR2 or TLR4) so as to prevent inappropriate immune responses against such commensal bacteria, which, it must be admitted, are seen in lesser quantities at the ocular surface than in the large intestine.

In support of our view are recent studies providing new evidence that intestinal epithelial cells, perhaps in a bid to create a quiescent condition, express extremely low levels of TLR4 and no MD-2, a critical coreceptor of TLR4, and therefore do not respond to LPS (13, 14). These findings contradict earlier reports, which demonstrated that intestinal epithelial cells expressed TLR4 and thus were activated by LPS (16, 17). It has also been shown that nondifferentiated T84 cells obtained from colon cancers did not respond to LPS, because TLR4 was expressed in the cytoplasmic compartment and not at the apical surface (15). In contrast, differentiated T84 cells expressing TLR4 at the apical surface were found to be capable of responding to LPS (15). Together with our results, these findings suggest that mucosal epithelial cells, which continuously interact with commensal bacteria, are capable of down-regulating the expression of TLR2 and TLR4. It is only natural that peripheral dendritic cells and macrophages, situated as they are in immunologically sanitary conditions, respond immediately to pathogen-associated molecules such as LPS via TLR4 to initiate immune responses. In contrast, epithelial cells, directly exposed as they are to external environmental Ags along with resident commensals, must behave in a totally different manner with regard to TLR-mediated immune responses. Moreover, on the ocular surface of humans, differentiated corneal and conjunctival epithelial cells are exposed to commensal bacteria and therefore would be expected to possess a down-regulatory mechanism for the TLR-mediated stimulation cascades. However, a previous report found just the opposite; human corneal epithelial cells were capable of responding to LPS via TLR4 expressed on their cell surface (37). One possible explanation could be that the previous study based its conclusion on the basis of a single line of corneal epithelial cells (10.014 pRSV-T) (37). In addition, another previous study demonstrated that human corneal epithelium were capable of responding to LPS, which resulted in the production of inflammatory cytokines (e.g., IL-1α) (38). Because this study used human corneal limbal epithelium cultured from explants prepared from limbal rings of donor cornea, one cannot neglect the possibility that other alien cells in the explant responded to LPS. To this end, corneal endothelial cells, keratocytes, and fibroblasts associated with oculus from human and animals have been shown to respond to LPS (39–42). Further a previous report showed that explants of corneal rims yielded in the outgrowth of epithelial cells together with some single or clustered spindle-shaped cells resembling fibroblasts (42). It has been also shown that endotoxin-induced keratitis occurred in mice after administration of LPS to cornea (43–45). However, it should be noted that LPS-induced keratitis only occurred when corneal epithelium was abraded. Although we cannot pinpoint the reason for this discrepancy with the previous studies, we believe that our results convincingly demonstrate that although the corneal epithelial cell line and primary corneal epithelial cells express TLR2 and TLR4 in the cytoplasm, they remain unresponsive to PGN and LPS, respectively, as evidenced by the lack of inflammatory cytokine production, mRNA expression, and NF-κB activity.

Our study also presents the novel finding that human corneal epithelial cells express TLR2 and TLR4 intracellularly, but not at the cell surface. Our experiments further show that even when stimulated with IL-1α or TNF-α, HCE express neither TLR2 nor TLR4 on their cell surface. However, such cytokine treatment did activate corneal epithelial cells by means of the activation of

FIGURE 6. HCE-T and primary human corneal epithelial cells fail to respond to LPS even when LPS is translocated into the cytoplasm. When cocultured with Alexa 488-LPS, human corneal epithelial cells did not internalize it (*d* and *h* of *A*), but monocytes did (*b* of *A*). To examine whether intracellular TLR4 of human corneal epithelial cells can respond to LPS, Alexa 488-LPS was translocated into HCE-T and primary human corneal epithelial cells using DOTAP liposomal transfection reagent. Although human corneal epithelial cells did not spontaneously take up Alexa 488-LPS from the culture medium, the cells coincubated with 1 μg/ml Alexa-LPS and 5 μl/ml DOTAP showed punctated fluorescein (*f* and *j* of *A*). Confocal scanning laser microscopy showed extensive Alexa 488-LPS loading in the cytoplasm of human corneal epithelial cells. SYTOX Orange nucleic acid stain was used for counterstaining. In some experiments HCE-T and primary human corneal epithelial cells were cultured in 24-well plates and, upon reaching subconfluence, were left untreated or were exposed to DOTAP (5 μl/ml) alone, DOTAP with Alexa-LPS (1000 ng/ml), or human IL-1α (10 ng/ml) for 24 h. The culture supernatants were then harvested for measurement of IL-6 and IL-8 (*B*). To examine NF-κB activation, HCE-T were plated in six-well plates and, upon reaching subconfluence, were left untreated or were exposed to DOTAP (5 μl/ml) alone, DOTAP with Alexa-LPS (1000 ng/ml), or human IL-1α (10 ng/ml) for 7 h. After the stimulation, the NF-κB assay was performed using TransAM (*C*). ELISA and NF-κB assay data represent the mean ± SEM from an experiment with triplicate wells. *, $p < 0.05$; **, $p < 0.005$; ***, $p < 0.0005$. Each bar represents a length of 50 μm.

NF-κB and the production of inflammatory cytokines, including IL-6 and IL-8. Thus, even when activated, human corneal epithelial cells did not recruit cytoplasmically expressed TLR4 to the cell surface. Further, our experiments showed that human corneal epithelial cells failed to respond to LPS even when LPS was artificially translocated into them. At the moment, we do not have any specific explanation for this unique finding. However, it was recently shown that a deficiency of MD-2, an associated molecule of the extracellular domain of TLR4, resulted in the lack of cell surface TLR4 expression (46). When embryonic fibroblasts from LPS-nonresponsive MD-$2^{-/-}$ mice were examined, it was discovered that TLR4 could not reach the plasma membrane, but instead accumulated predominantly in the Golgi apparatus. In contrast, TLR4 was distributed at the leading edge surface of cells in wild-type embryonic fibroblasts (46). Moreover, TLRs were shown to be retained intracellularly in the absence of endoplasmic reticulum chaperone gp96, and thus the mutant cells of gp96 deficiency did not respond to microbial stimuli (47). Based on these results, it would seem plausible that cell surface TLR expression could be regulated at the level of TLR4-associated molecules (e.g., MD-2) and chaperon. These interesting possibilities will, of course, be the subject of our future investigations.

In summary, the data presented in this study demonstrate that human corneal epithelial cells fail to respond to PGN and LPS due to their inability to express TLR2 and TLR4, respectively, on their cell surfaces. Although both TLR2 and TLR4 were observed in the cytoplasm of human corneal epithelial cells, translocation of LPS to the cytoplasm did not elicit a response by those cells. These findings suggest that human corneal epithelial cells possess a unique regulatory mechanism for the inhibition of TLR2- and TLR4-mediated innate immunity.

Acknowledgments

We thank S. Terawaki and the members of Department of Mucosal Immunology, Osaka University, and Division of Mucosal Immunology, University of Tokyo, for their helpful discussions and suggestions. We also thank Drs. S. Akashi and K. Miyake (University of Tokyo) for their helpful discussions and suggestions.

References

1. Haynes, R. J., P. J. Tighe, and H. S. Dua. 1999. Antimicrobial defensin peptides of the human ocular surface. *Br. J. Ophthalmol. 83:737.*
2. Aswad, M. I., T. John, M. Barza, K. Kenyon, and J. Baum. 1990. Bacterial adherence to extended wear soft contact lenses. *Ophthalmology 97:296.*
3. Gudmundsson, O. G., L. D. Ormerod, K. R. Kenyon, R. J. Glynn, A. S. Baker, J. Haaf, S. Lubars, M. B. Abelson, S. A. Boruchoff, C. S. Foster, et al. 1989. Factors influencing predilection and outcome in bacterial keratitis. *Cornea 8:115.*
4. Doyle, A., B. Beigi, A. Early, A. Blake, P. Eustace, and R. Hone. 1995. Adherence of bacteria to intraocular lenses: a prospective study. *Br. J. Ophthalmol. 79:347.*
5. Hara, J., F. Yasuda, and M. Higashitsutsumi. 1997. Preoperative disinfection of the conjunctival sac in cataract surgery. *Ophthalmologica 211(Suppl. 1):62.*
6. Lemaitre, B., E. Nicolas, L. Michaut, J. M. Reichhart, and J. A. Hoffmann. 1996. The dorsoventral regulatory gene cassette spatzle/Toll/cactus controls the potent antifungal response in *Drosophila* adults. *Cell 86:973.*
7. Medzhitov, R., P. Preston-Hurlburt, and C. A. Janeway, Jr. 1997. A human homologue of the *Drosophila* Toll protein signals activation of adaptive immunity. *Nature 388:394.*
8. Medzhitov, R., and C. Janeway, Jr. 2000. Innate immune recognition: mechanisms and pathways. *Immunol. Rev. 173:89.*
9. Poltorak, A., X. He, I. Smirnova, M. Y. Liu, C. Van Huffel, X. Du, D. Birdwell, E. Alejos, M. Silva, C. Galanos, et al. 1998. Defective LPS signaling in C3H/HeJ and C57BL/10ScCr mice: mutations in Tlr4 gene. *Science 282:2085.*
10. Takeuchi, O., K. Hoshino, T. Kawai, H. Sanjo, H. Takada, T. Ogawa, K. Takeda, and S. Akira. 1999. Differential roles of TLR2 and TLR4 in recognition of Gram-negative and Gram-positive bacterial cell wall components. *Immunity 11:443.*
11. Schwandner, R., R. Dziarski, H. Wesche, M. Rothe, and C. J. Kirschning. 1999. Peptidoglycan- and lipoteichoic acid-induced cell activation is mediated by Toll-like receptor 2. *J. Biol. Chem. 274:17406.*
12. Hornung, V., S. Rothenfusser, S. Britsch, A. Krug, B. Jahrsdorfer, T. Giese, S. Endres, and G. Hartmann. 2002. Quantitative expression of Toll-like receptor 1–10 mRNA in cellular subsets of human peripheral blood mononuclear cells and sensitivity to CpG oligodeoxynucleotides. *J. Immunol. 168:4531.*
13. Abreu, M. T., P. Vora, E. Faure, L. S. Thomas, E. T. Arnold, and M. Arditi. 2001. Decreased expression of Toll-like receptor-4 and MD-2 correlates with intestinal epithelial cell protection against dysregulated proinflammatory gene expression in response to bacterial lipopolysaccharide. *J. Immunol. 167:1609.*
14. Abreu, M. T., E. T. Arnold, L. S. Thomas, R. Gonsky, Y. Zhou, B. Hu, and M. Arditi. 2002. TLR4 and MD-2 expression is regulated by immune-mediated signals in human intestinal epithelial cells. *J. Biol. Chem. 277:20431.*
15. Cario, E., D. Brown, M. McKee, K. Lynch-Devaney, G. Gerken, and D. K. Podolsky. 2002. Commensal-associated molecular patterns induce selective Toll-like receptor-trafficking from apical membrane to cytoplasmic compartments in polarized intestinal epithelium. *Am. J. Pathol. 160:165.*
16. Cario, E., I. M. Rosenberg, S. L. Brandwein, P. L. Beck, H. C. Reinecker, and D. K. Podolsky. 2000. Lipopolysaccharide activates distinct signaling pathways in intestinal epithelial cell lines expressing Toll-like receptors. *J. Immunol. 164:966.*
17. Hornef, M. W., T. Frisan, A. Vandewalle, S. Normark, and A. Richter-Dahlfors. 2002. Toll-like receptor 4 resides in the Golgi apparatus and colocalizes with internalized lipopolysaccharide in intestinal epithelial cells. *J. Exp. Med. 195:559.*
18. Becker, M. N., G. Diamond, M. W. Verghese, and S. H. Randell. 2000. CD14-dependent lipopolysaccharide-induced β-defensin-2 expression in human tracheobronchial epithelium. *J. Biol. Chem. 275:29731.*
19. Wolfs, T. G., W. A. Buurman, A. van Schadewijk, B. de Vries, M. A. Daemen, P. S. Hiemstra, and C. van't Veer. 2002. In vivo expression of Toll-like receptor 2 and 4 by renal epithelial cells: IFN-γ and TNF-α mediated up-regulation during inflammation. *J. Immunol. 168:1286.*
20. Schilling, J. D., M. A. Mulvey, C. D. Vincent, R. G. Lorenz, and S. J. Hultgren. 2001. Bacterial invasion augments epithelial cytokine responses to *Escherichia coli* through a lipopolysaccharide-dependent mechanism. *J. Immunol. 166:1148.*
21. Backhed, F., M. Soderhall, P. Ekman, S. Normark, and A. Richter-Dahlfors. 2001. Induction of innate immune responses by *Escherichia coli* and purified lipopolysaccharide correlate with organ- and cell-specific expression of Toll-like receptors within the human urinary tract. *Cell. Microbiol. 3:153.*
22. Uehara, A., S. Sugawara, and H. Takada. 2002. Priming of human oral epithelial cells by interferon-γ to secrete cytokines in response to lipopolysaccharides, lipoteichoic acids and peptidoglycans. *J. Med. Microbiol. 51:626.*
23. Uehara, A., S. Sugawara, R. Tamai, and H. Takada. 2001. Contrasting responses of human gingival and colonic epithelial cells to lipopolysaccharides, lipoteichoic acids and peptidoglycans in the presence of soluble CD14. *Med. Microbiol. Immunol. 189:185.*
24. Krisanaprakornkit, S., J. R. Kimball, A. Weinberg, R. P. Darveau, B. W. Bainbridge, and B. A. Dale. 2000. Inducible expression of human β-defensin 2 by *Fusobacterium nucleatum* in oral epithelial cells: multiple signaling pathways and role of commensal bacteria in innate immunity and the epithelial barrier. *Infect. Immun. 68:2907.*
25. Araki-Sasaki, K., Y. Ohashi, T. Sasabe, K. Hayashi, H. Watanabe, Y. Tano, and H. Handa. 1995. An SV40-immortalized human corneal epithelial cell line and its characterization. *Invest. Ophthalmol. Vis. Sci. 36:614.*
26. Jumblatt, M. M., and A. H. Neufeld. 1983. β-Adrenergic and serotonergic responsiveness of rabbit corneal epithelial cells in culture. *Invest. Ophthalmol. Vis. Sci. 24:1139.*
27. Hayashida-Hibino, S., H. Watanabe, K. Nishida, M. Tsujikawa, T. Tanaka, Y. Hori, Y. Saishin, and Y. Tano. 2001. The effect of TGF-β1 on differential gene expression profiles in human corneal epithelium studied by cDNA expression array. *Invest. Ophthalmol. Vis. Sci. 42:1691.*
28. Ohta, N., T. Hiroi, M. N. Kweon, N. Kinoshita, Jang, M. H., T. Mashimo, J. Miyazaki, and H. Kiyono. 2002. IL-15-dependent activation-induced cell death-resistant Th1 type CD8 $\alpha\beta^+$NK1.1$^+$ T cells for the development of small intestinal inflammation. *J. Immunol. 169:460.*
29. Takeuchi, O., K. Takeda, K. Hoshino, O. Adachi, T. Ogawa, and S. Akira. 2000. Cellular responses to bacterial cell wall components are mediated through MyD88-dependent signaling cascades. *Int. Immunol. 12:113.*
30. Yura, M., I. Takahashi, M. Serada, T. Koshio, K. Nakagami, Y. Yuki, and H. Kiyono. 2001. Role of MOG-stimulated Th1 type "light up" (GFP$^+$) CD4$^+$ T cells for the development of experimental autoimmune encephalomyelitis (EAE). *J. Autoimmun. 17:17.*
31. Renard, P., I. Ernest, A. Houbion, M. Art, H. Le Calvez, M. Raes, and J. Remacle. 2001. Development of a sensitive multi-well colorimetric assay for active NFκB. *Nucleic Acids Res. 29:E21.*
32. Eldstrom, J. R., K. La, and D. A. Mathers. 2000. Polycationic lipids translocate lipopolysaccharide into HeLa cells. *BioTechniques 28:510.*
33. Dana, M. R. 2004. Corneal antigen-presenting cells: diversity, plasticity, and disguise: the Cogan lecture. *Invest. Ophthalmol. Vis. Sci. 45:722.*
34. Kim, J. M., L. Eckmann, T. C. Savidge, D. C. Lowe, T. Witthoft, and M. F. Kagnoff. 1998. Apoptosis of human intestinal epithelial cells after bacterial invasion. *J. Clin. Invest. 102:1815.*
35. Mowat, A. M. 2003. Anatomical basis of tolerance and immunity to intestinal antigens. *Nat. Rev. Immunol. 3:331.*
36. Hentschel, U., U. Dobrindt, and M. Steinert. 2003. Commensal bacteria make a difference. *Trends Microbiol. 11:148.*
37. Song, P. I., T. A. Abraham, Y. Park, A. S. Zivony, B. Harten, H. F. Edelhauser,

S. L. Ward, C. A. Armstrong, and J. C. Ansel. 2001. The expression of functional LPS receptor proteins CD14 and Toll-like receptor 4 in human corneal cells. *Invest. Ophthalmol. Vis. Sci. 42:2867.*

38. Solomon, A., M. Rosenblatt, D. Li, Z. Liu, D. Monroy, Z. Ji, B. Lokeshwar, and S. Pflugfelder. 2000. Doxycycline inhibition of interleukin-1 in the corneal epithelium. *Invest. Ophthalmol. Vis. Sci. 41:2544.*
39. Del Vecchio, P. J., and J. B. Shaffer. 1991. Regulation of antioxidant enzyme expression in LPS-treated bovine retinal pigment epithelial and corneal endothelial cells. *Curr. Eye Res. 10:919.*
40. Dighiero, P., F. Behar-Cohen, Y. Courtois, and O. Goureau. 1997. Expression of inducible nitric oxide synthase in bovine corneal endothelial cells and keratocytes in vitro after lipopolysaccharide and cytokines stimulation. *Invest. Ophthalmol. Vis. Sci. 38:2045.*
41. Sekine-Okano, M., R. Lucas, D. Rungger, T. De Kesel, G. E. Grau, P. M. Leuenberger, and E. Rungger-Brandle. 1996. Expression and release of tumor necrosis factor-α by explants of mouse cornea. *Invest. Ophthalmol. Vis. Sci. 37:1302.*
42. Shams, N. B. K., M. M. Sigel, and R. M. Davis. 1989. Interferon-γ, *Staphylococcus aureus*, and lipopolysaccharide/silica enhance interleukin-1β production by human corneal cells. *Reg. Immunol. 2:136.*
43. Schultz, C. L., D. W. Morck, S. G. McKay, M. E. Olson, and A. Buret. 1997. Lipopolysaccharide induced acute red eye and corneal ulcers. *Exp Eye Res. 64:3.*
44. Khatri, S., J. H. Lass, F. P. Heinzel, W. M. Petroll, J. Gomez, E. Diaconu, C. M. Kalsow, and E. Pearlman. 2002. Regulation of endotoxin-induced keratitis by PECAM-1, MIP-2, and Toll-like receptor 4. *Invest. Ophthalmol. Vis. Sci. 43:2278.*
45. Schultz, C. L., A. G. Buret, M. E. Olson, H. Ceri, R. R. Read, and D. W. Morck. 2000. Lipopolysaccharide entry in the damaged cornea and specific uptake by polymorphonuclear neutrophils. *Infect. Immun. 68:1731.*
46. Nagai, Y., S. Akashi, M. Nagafuku, M. Ogata, Y. Iwakura, S. Akira, T. Kitamura, A. Kosugi, M. Kimoto, and K. Miyake. 2002. Essential role of MD-2 in LPS responsiveness and TLR4 distribution. *Nat. Immunol. 3:667.*
47. Randow, F., and B. Seed. 2001. Endoplasmic reticulum chaperone gp96 is required for innate immunity but not cell viability. *Nat. Cell. Biol. 3:891.*

Available online at www.sciencedirect.com
SCIENCE DIRECT®
Biochemical and Biophysical Research Communications 315 (2004) 356–362
BBRC
www.elsevier.com/locate/ybbrc

Roles of a conserved family of adaptor proteins, Lnk, SH2-B, and APS, for mast cell development, growth, and functions: *APS*-deficiency causes augmented degranulation and reduced actin assembly

Chiyomi Kubo-Akashi, Masanori Iseki, Sang-Mo Kwon, Hitoshi Takizawa, Kiyoshi Takatsu,* and Satoshi Takaki*

Division of Immunology, Department of Microbiology and Immunology, The Institute of Medical Science, The University of Tokyo, Shirokanedai 4-6-1, Minato-ku, Tokyo 108-8639, Japan

Received 18 December 2003

Abstract

Lnk, SH2-B, and APS form a conserved adaptor protein family. All of those proteins are expressed in mast cells and their possible functions in signaling through c-Kit or FcεRI have been speculated. To investigate roles of Lnk, SH2-B or APS in mast cells, we established IL-3-dependent mast cells from *lnk*$^{-/-}$, *SH2-B*$^{-/-}$, and *APS*$^{-/-}$ mice. IL-3-dependent growth of those cells was comparable. Proliferation or adhesion mediated by c-Kit as well as degranulation induced by cross-linking FcεRI were normal in the absence of Lnk or SH2-B. In contrast, *APS*-deficient mast cells showed augmented degranulation after cross-linking FcεRI compared to wild-type cells, while c-Kit-mediated proliferation and adhesion were kept unaffected. *APS*-deficient mast cells showed reduced actin assembly at steady state, although their various intracellular responses induced by cross-linking FcεRI were indistinguishable compared to wild-type cells. Our results suggest potential roles of APS in controlling actin cytoskeleton and magnitude of degranulation in mast cells.

Keywords: Actin cytoskeleton; Adaptor protein; BMMC; c-Kit; Cytokine; Cytokine receptor; Degranulation; FcεRI; IgE; Signal transduction; Tyrosine kinase

Mast cells play critical roles in allergic and inflammatory responses. Mast cells express the high affinity IgE receptor FcεRI and cross-linking of IgE bound to FcεRI by antigens initiates a series of molecular events in mast cells, which lead to degranulation and release of a wide variety of chemical mediators such as histamine, arachidonic acid metabolites, and soluble proteins including neutral proteases and cytokines [1–3]. Even in the absence of antigen, binding of monomeric IgE to FcεRI induces cytokine production and cell survival [4]. Mast cells differentiate from hematopoietic progenitor cells. Stem cell factor (SCF), which is also known as mast cell growth factor, and IL-3 provide signals for their differentiation, proliferation, and survival mediated through c-Kit receptor tyrosine kinase and IL-3 receptor, respectively. SCF also regulates chemotaxis and adhesion of mature mast cells [1,5].

Lnk, SH2-B, and APS form a conserved family of adaptor proteins, whose members share a homologous N-terminal region with proline rich stretches, PH and SH2 domains, and a conserved C-terminal tyrosine phosphorylation site [6–9]. Lnk plays a critical role in regulating production of B cell precursors and hematopoietic progenitor cells, and functions as a negative regulator of c-Kit-mediated signaling. We have shown that *lnk*$^{-/-}$ mice show enhanced B cell production because of the hypersensitivity of B cell precursors to SCF [8]. In addition, *lnk*$^{-/-}$ mice exhibit increased numbers of hematopoietic progenitors in the bone marrow, and the ability of hematopoietic progenitors to repopulate

* Corresponding authors. Fax: +81-3-5449-5407.
E-mail addresses: takatsuk@ims.u-tokyo.ac.jp (K. Takatsu), takakis@ims.u-tokyo.ac.jp (S. Takaki).

0006-291X/$ - see front matter © 2004 Elsevier Inc. All rights reserved.
doi:10.1016/j.bbrc.2004.01.060

irradiated host animals was greatly enhanced by the absence of Lnk [10]. Independently, Velazquez et al. [11] have reported *lnk*-deficiency results in abnormal modulation of SCF and IL-3-mediated signaling pathways and augmented growth of bone marrow cells or splenocytes. SH2-B is originally identified as a protein associated with immunoreceptor tyrosine-based activation motifs (ITAMs) of FcεRI γ-chain by a modified two-hybrid (tribrid system) screening [6]. We have shown that SH2-B is a critical molecule for the maturation of reproduction organs that is at least in part mediated by insulin-like growth factor I (IGF-I) receptor signaling [12]. APS is identified as a potential substrate of c-Kit by two-hybrid system [7]. We also independently isolated the murine counterpart of APS as a protein homologous to Lnk and SH2-B [9]. APS is phosphorylated upon stimulation with various growth factors, including EPO-R, PDGF-R, insulin, nerve growth factor (NGF), and cross-linking B cell receptor (BCR) [9,13–16]. Recently, we generated *APS*$^{-/-}$ mice and found that B-1 cells in peritoneal cavity were increased, and humoral immune responses to type-2 antigen significantly enhanced in *APS*$^{-/-}$ mice [17].

Lnk-family adaptor proteins, Lnk, SH2-B, and APS, are all expressed in bone marrow-derived mast cells (BMMCs) [12]. In addition, various experiments using cell lines overexpressing those Lnk-family adaptor proteins suggested their possible functions in signaling mediated through c-Kit or FcεRI. We investigated and compared for the first time consequences of the deficiency either of Lnk, SH2-B or APS in mast cell functions using primary cultured cells. We established BMMCs from bone marrow progenitors of *lnk*$^{-/-}$, *SH2-B*$^{-/-}$, *APS*$^{-/-}$ mice, and their respective control wild-type mice. IL-3-dependent BMMCs were equally established even in the absence of Lnk, SH2-B or APS. SCF-dependent proliferation or adhesion was also not compromised and was comparable among *lnk*$^{-/-}$, *SH2-B*$^{-/-}$, and *APS*$^{-/-}$ BMMCs. Although FcεRI-mediated degranulation was not affected by the absence of Lnk or SH2-B, *APS*$^{-/-}$ BMMCs showed enhanced degranulation after cross-linking FcεRI. *APS*$^{-/-}$ BMMCs showed reduced filamentous actin (F-actin) assembly at steady state and was resistant to inhibitors disrupting F-actin microfilaments in FcεRI-mediated degranulation responses. These results suggest that APS plays a role in negative regulation of mast cell degranulation by controlling actin dynamics.

Materials and methods

Cells and culture. Bone marrow cells were obtained from 8- to 10-week-old *lnk*$^{-/-}$ [8], *SH2-B*$^{-/-}$ [12], *APS*$^{-/-}$ mice [17], and their respective wild-type littermates, and cultured in RPMI1640 supplemented with 5 ng/ml murine IL-3 (PeproTech), 8% fetal calf serum (FCS), nonessential amino acids (Gibco-BRL), 100 IU/ml penicillin, 100 μg/ml streptomycin, and 10 μM of 2-mercaptoethanol. Cells were split and supplied with fresh medium every 4 or 5 days. After 4 weeks of cultivation, greater than 95% of cells were c-Kit and FcεRI positive as assessed by flow cytometry.

Flow cytometry and cytochemistry. For the detection of FcεRI, BMMCs were incubated in a supernatant of IGEL a2 (15.3) hybridoma containing mouse anti-DNP IgE monoclonal antibody (mAb) and then stained with fluorescein isothiocyanate (FITC)-conjugated anti-mouse IgE mAb (LO-ME-2, Oxford Biomarketing, UK). For the detection of c-Kit, cells were stained with phycoerythrin (PE)-conjugated anti-CD117 mAb (2B8, Pharmingen). For measurements of F-actin content, cells were fixed in 3.7% formaldehyde for 6 h at 4 °C permeabilized with 0.2% Triton X-100 in PBS for 30 min and then stained with rhodamine-conjugated phalloidin (Molecular Probes, Eugene, OR) for 1 h. Stained cells were then analyzed by flow cytometry using a FACSCalibur (Becton–Dickinson).

Unstimulated or stimulated BMMCs were resuspended in PBS and deposited onto microscope slides using a Cytospin 3 (Shandon Scientific, Cheshire, England). After staining with May–Gruenwald's and Giemsa's solutions (MERCK), cellular morphology was assessed by a light microscope.

Proliferation and survival assays. BMMCs (5×10^4) were cultured in 0.2 ml of flesh medium containing various concentrations of SCF (PeproTech) in a 96-well multi-well plate for 72 h. Cells were pulsed with [^{3}H]thymidine (0.2 μCi/well) in the last 12 h of culture and harvested and incorporated [^{3}H]thymidine was measured in triplicate determination using a MATRIX 96 Direct Beta Counter (Packard, Meriden, CT). Cells were cultured in media alone or in the presence of various concentrations of anti-DNP IgE mAb (SPE-7, Sigma). Percentage of viable cells was determined by trypan blue exclusion.

Adhesion assay. Adhesion assays to fibronectin were performed as previously described [18]. In brief, 5×10^4 BMMCs labeled with 2′,7′-bis-(2-carboxyethyl)-5-(and-6)-carboxy fluorescein (BCECF: Molecular Probes, Eugene, OR) were incubated in triplicate in a 96-well polystyrene plate (Lynbro-Titertek, Aurora, OH) coated with fibronectin (Sigma) in the presence of various concentrations of SCF or 10 ng/ml PMA at 37 °C for 30 min. Unbound cells were removed by washing the plates with binding medium RPMI 1640 containing 10 mM Hepes (pH 7.4), and 0.03% BSA four times. Adhered cells were quantified by measuring fluorescence of input and bound cells using a Fluorescence Concentration Analyzer (IDEXX Laboratories, Westbrook, ME).

Degranulation assay. BMMCs were sensitized with anti-DNP IgE at 37 °C for 18 h, washed, and resuspended in Tyrode's buffer (10 mM Hepes, pH 7.4, 130 mM NaCl, 5 mM KCl, 1.4 mM $CaCl_2$, 1 mM $MgCl_2$, 5.6 mM glucose, and 0.1% BSA). Cells (5×10^5 in 0.2 ml) were then stimulated with various concentrations of DNP-BSA or 10 ng/ml PMA plus 400 ng/ml ionomycin at 37 °C for 1 h. Enzymatic activities of β-hexosaminidase in supernatants and cells solubilized in 0.5% Triton X-100 Tyrode's buffer were measured using *p*-nitrophenyl *N*-acetyl-β-D-glucosaminidase (Sigma) as substrates. Degranulation was calculated as the percentage of β-hexosaminidase released from cells in the total amount of the enzyme in the supernatants and cell pellets as described before [18]. For the experiment using latrunculin, sensitized BMMCs were pretreated with various concentrations of latrunculin for 15 min at 37 °C before assays. Histamine released into culture supernatants after degranulation was measured using ELISA kit (Immunotech, Marseille, France) according to manufacturer's recommendation.

Calcium measurements. Sensitized BMMCs were incubated with 6 μM Fura PE3/AM (TEFLABS, Austin, TX) in PBS containing 20 mM Hepes (pH 7.4), 5 mM glucose, 0.025% BSA, and 1 mM $CaCl_2$ (HBS) at 37 °C for 60 min. Cells were washed and resuspended in HBS (1×10^5 cells/0.1 ml) in a stirring cuvette. Fluorescence was monitored continuously with a fluorescence spectrophotometer (CAF-110: JASCO, Osaka, Japan) at an emission wavelength of 500 nm and two different excitation wavelengths (340 and 380 nm).

Immunoblotting. Cell lysates from stimulated BMMCs were subjected to immunoprecipitation and Western blot analysis as previously

described [9]. The proteins were resolved by SDS–8% PAGE and transferred to PVDF membranes (Immobilon, Millipore). After blocking with 5% BSA, membranes were probed with anti-phosphotyrosine mAb (4G10, Upstate Biotechnology) and incubated with HRP-conjugated secondary antibodies. Blots were washed in 0.05% Tween 20/Tris-buffered saline, pH 7.6, and proteins were detected by chemiluminescence (Perkin–Elmer Life Sciences).

Results

Establishment of BMMCs lacking either Lnk, SH2-B or APS

Lnk, SH2-B, and APS were all expressed in normal BMMCs [12]. To investigate possible functions of those adaptor proteins in mast cells, we established IL-3-dependent BMMCs from bone marrow progenitors of *lnk*$^{-/-}$, *SH2-B*$^{-/-}$, and *APS*$^{-/-}$ mice and their responses were compared with those of BMMCs established from respective control wild-type littermates. IL-3-dependent growth of *lnk*$^{-/-}$, *SH2-B*$^{-/-}$ or *APS*$^{-/-}$ bone marrow progenitor cells was almost comparable to that of respective control progenitor cells (Fig. 1A). Established *lnk*$^{-/-}$, *SH2-B*$^{-/-}$ or *APS*$^{-/-}$ BMMCs were not distinguishable from the wild-type BMMCs in terms of surface expression of FcεRI and c-Kit (Fig. 1B). Mast cell differentiation and proliferation induced by IL-3 was not affected at all even in the absence of Lnk, SH2-B or APS.

Functions of lnk$^{-/-}$, *SH2-B*$^{-/-}$ *or APS*$^{-/-}$ *BMMCs*

First, we examined proliferative responses of established BMMCs to SCF and found no difference among *lnk*$^{-/-}$, *SH2-B*$^{-/-}$, *APS*$^{-/-}$, and respective control BMMCs (Fig. 2A). Adhesion to fibronectin induced by SCF or PMA was also not affected in the absence of Lnk, SH2-B or APS (Fig. 2B). We then examined degranulation of those BMMCs induced by cross-linking FcεRI by measuring β-hexosaminidase and histamine released after stimulation. Degranulation from *lnk*$^{-/-}$ or *SH2-B*$^{-/-}$ BMMCs was almost comparable to that from control wild-type BMMCs (Fig. 2C). In contrast, *APS*$^{-/-}$ BMMCs showed enhanced degranulation responses upon cross-linking FcεRI (Fig. 2C). Degranulation from *APS*$^{-/-}$ BMMCs, determined by β-hexosaminidase releasability, was 130–140% of that from control cells at each stimulation condition, and the enhancement was statistically significant at the concentrations of DNP-BSA over 0.5 μg/ml (Table 1). Histamine released after cross-linking FcεRI was also augmented in *APS*$^{-/-}$ BMMCs (data not shown).

FcεRI-mediated cellular responses in APS$^{-/-}$ *BMMCs*

To clarify the possible molecular mechanisms leading to the enhanced degranulation in the absence of APS,

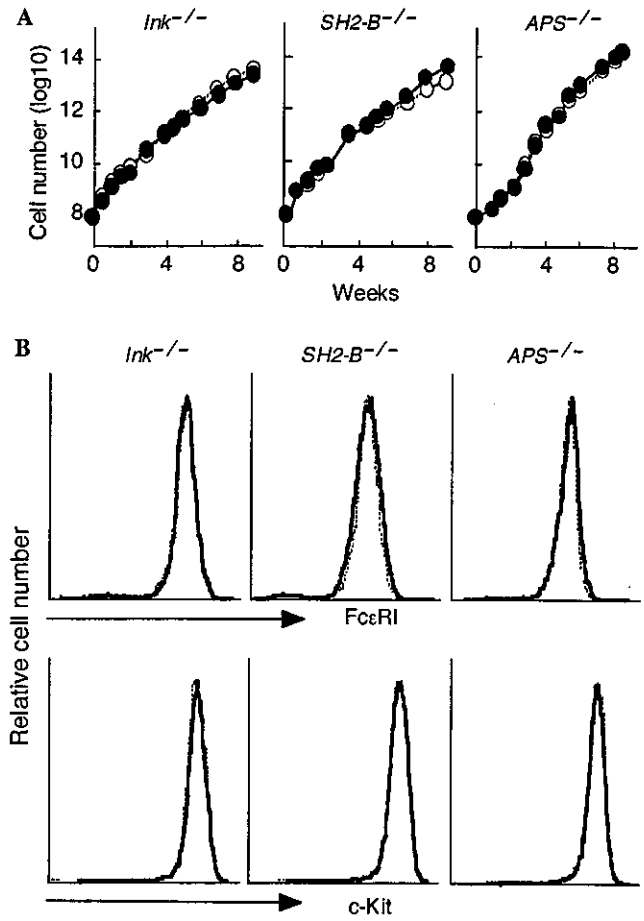

Fig. 1. (A) Cumulative cell numbers of *lnk*$^{-/-}$, *SH2-B*$^{-/-}$, *APS*$^{-/-}$ (closed circles), and respective wild-type control (open circles) BMMCs. Differentiation of BMMCs from progenitors and their cell growth induced by IL-3 was comparable in the absence of either Lnk, SH2-B or APS. Representative results obtained from multiple independent pairs of BMMCs are shown. (B) Surface expressions of FcεRI (upper panels) or c-Kit (lower panels) on *lnk*$^{-/-}$, *SH2-B*$^{-/-}$, *APS*$^{-/-}$ (bold lines), and respective wild-type control (dotted lines) BMMCs. After IgE sensitization, BMMCs were stained with anti-c-Kit or anti-IgE antibodies and analyzed by flow cytometry. Representative results of multiple independent experiments are shown.

we tried to evaluate various cellular events induced by cross-linking FcεRI. We first cytochemically evaluated the proportion of degranulated BMMCs after stimulation. Percentage of degranulated cells increased in a dose-dependent manner as the concentration of antigens increased. Importantly, the ratio of degranulated BMMCs in each stimulation condition was comparable between *APS*$^{-/-}$ and wild-type BMMCs (Fig. 3A). The enhanced degranulation from *APS*$^{-/-}$ BMMCs was thus due to augmented degranulation from each mast cell but not to increased proportion of cells that underwent degranulation. We then analyzed calcium influx induced by cross-linking FcεRI, however, we did not observe significant difference in initial peak and following sustained increase of intracellular free calcium between *APS*$^{-/-}$ and control BMMCs (Fig. 3B). Cell survival

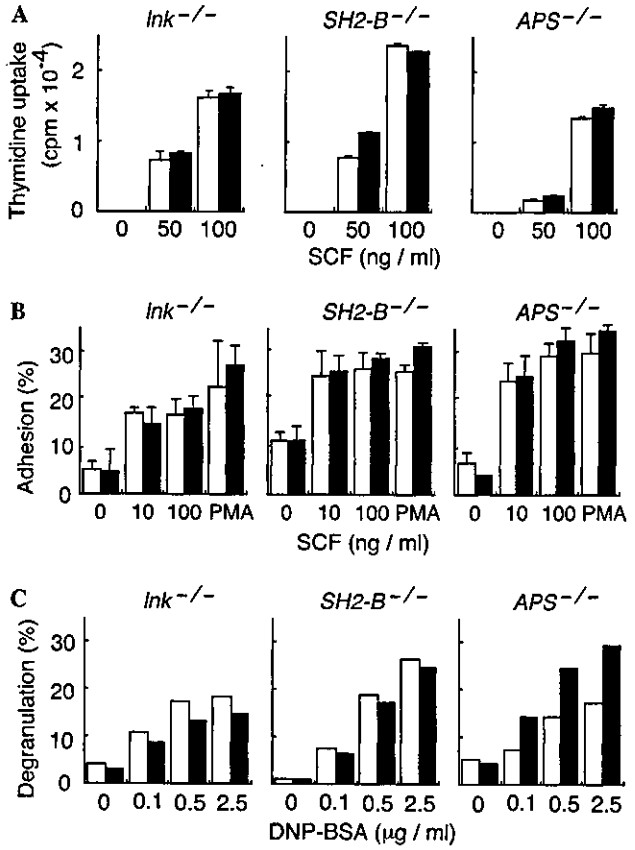

Fig. 2. Responses of *lnk*$^{-/-}$, *SH2-B*$^{-/-}$ or *APS*$^{-/-}$ BMMCs (filled bars) and of respective control BMMCs (open bars) induced by activation of c-Kit or FcεRI. (A) Proliferation upon stimulation with various concentrations of SCF. Values shown are the mean cpm ± SD of triplicate determinations. (B) Adhesion to fibronectin induced by various concentrations of SCF or 10 ng/ml PMA. Shown are average ± SD of triplicate measurements. (C) Degranulation after cross-linking FcεRI. Cells sensitized with anti-DNP IgE mAb were stimulated with the various concentrations of DNP-BSA. Shown is the percentage of β-hexosaminidase activity released into culture supernatants out of the total β-hexosaminidase initially stored in cells. *APS*$^{-/-}$ BMMCs showed augmented degranulation responses (see also Table 1). Representative results of three independent experiments are shown from (A) through (C).

mediated by binding of monomeric IgE to FcεRI was also comparable (Fig. 3C). Tyrosine phosphorylation of various cellular proteins was rapidly induced after cross-linking FcεRI in mast cells and was comparable between *APS*$^{-/-}$ and wild-type BMMCs. Phosphorylation of neither Akt nor PKCδ molecules was affected in the absence of APS (data not shown).

Decreased actin assembly in APS$^{-/-}$ *BMMCs*

It has been shown that Lnk associates with an actin binding protein ABP-280 [19] and that SH2-B plays a role in actin reorganization and cell motility mediated by growth hormone receptor [20,21]. We recently found that Lnk facilitates actin reorganization in transfected fibroblast cells (S.M.K. and S.T., unpublished data). In addition, a negative correlation between actin polymerization and FcεRI-mediated degranulation from RBL-2H3 mast cell line has been presented [22,23].

We speculated APS may regulate actin cytoskeleton, which potentially has regulatory process for degranulation in mast cells. Therefore, we investigated consequences of inhibition of actin polymerization induced by cross-linking FcεRI in BMMCs and its effect on degranulation by treatment with latrunculin. Treatment of sensitized BMMCs with latrunculin resulted in the reduction of F-actin contents as demonstrated by rhodamine–phalloidine binding (Fig. 4A, left panel). Cross-linking FcεRI induced reduction of F-actin contents in stimulated BMMCs. Consistent with observations using RBL-2H3 cells, inhibition of actin assembly by treatment with latrunculin enhanced degranulation from normal BMMCs in a dose-dependent manner (Fig. 4A, right). Interestingly, sensitized *APS*$^{-/-}$ BMMCs showed reduced F-actin content (about 70% of control) compared to wild-type cells (Fig. 4B, left). The reduction in F-actin contents became less evident in cells treated with latrunculin. Finally, the effect of latrunculin on degranulation was compared between *APS*$^{-/-}$ and control BMMCs. As shown in Fig. 4B, augmented degranulation by *APS*$^{-/-}$ BMMCs became less evident by treatment with latrunculin, which was well correlated with difference in F-actin contents between latrunculin treated *APS*$^{-/-}$ and control cells. These results suggested that *APS*-deficiency in mast cells made actin assembly at relatively low levels and that resulted in facilitated degranulation process after cross-linking FcεRI.

Table 1
Enhancement of FcεRI-induced degranulation in *APS*$^{-/-}$ BMMC

DNP-BSA(μg/ml)	Degranulation (% maximal response induced by PMA plus ionomycin)			
	0	0.1	0.5	2.5
+/+ ($n = 11$)	5.6 ± 0.9	19.4 ± 2.4	28.9 ± 2.5	29.4 ± 2.1
−/− ($n = 11$)	5.0 ± 0.7	25.8 ± 3.9	39.5 ± 3.9*	40.6 ± 3.4**
(% +/+ response)	(89%)	(133%)	(136%)	(138%)

Sensitized BMMCs were stimulated with the various concentrations of DNP-BSA or 10 ng/ml PMA plus 400 ng/ml ionomycin. Values represent the mean ± SE of % β-hexosaminidase activity normalized by the value induced with PMA plus ionomycin as 100%. *$p < 0.05$, **$p < 0.01$ compared to +/+ BMMCs by Student's t test.

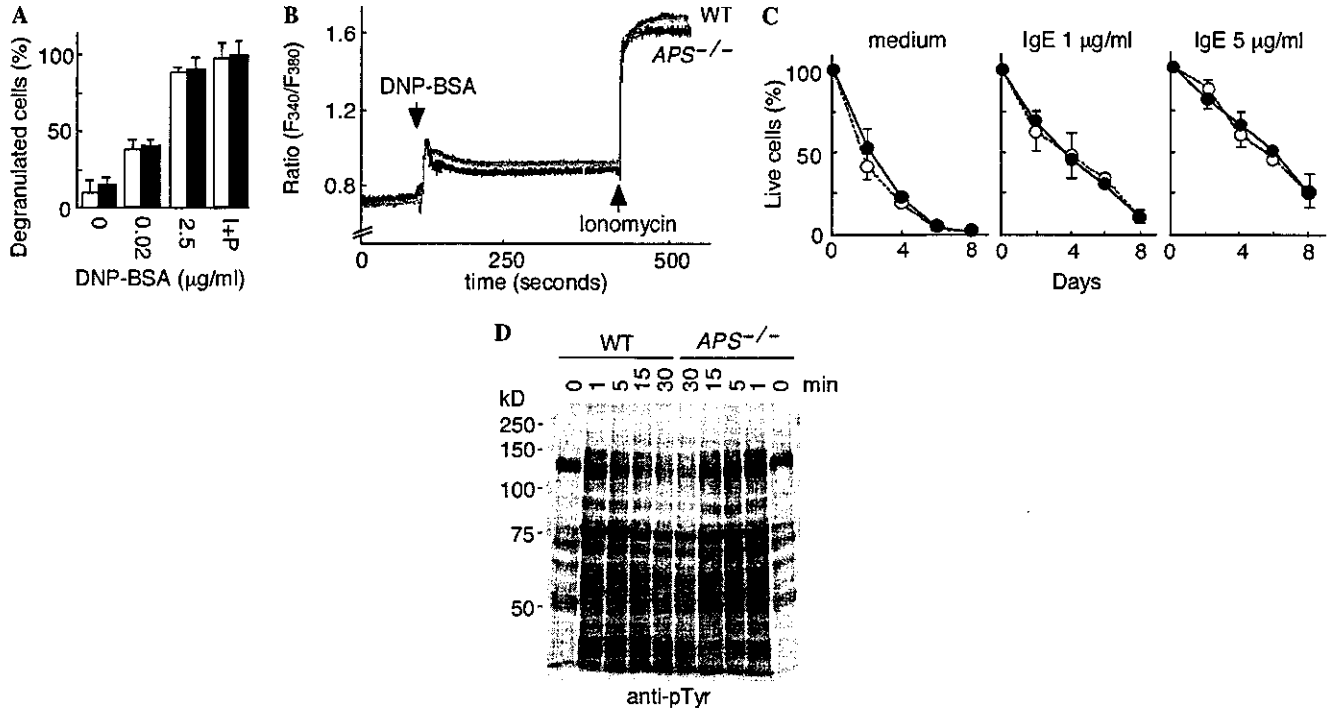

Fig. 3. Cellular responses of $APS^{-/-}$ BMMCs mediated through cross-linking FcεRI. (A) Proportion of degranulated cells after cross-linking FcεRI with various concentrations of antigens was determined by cytochemistry. Percentages of degranulated cells were comparable between $APS^{-/-}$ (closed bars) and wild-type control mice (open bars). The average ± SD of three independent experiments are shown. (B) Calcium influx induced upon cross-linking FcεRI in $APS^{-/-}$ (lower line) and wild-type (upper line) BMMCs. After IgE sensitization, BMMCs were loaded with Fura PE3 and stimulated with 5 μg/ml DNP-BSA and 10 μg/ml ionomycin at the indicated time points (arrows), and fluorescence intensity ratio at 340–380 nm was measured. Representative results of two independent experiments are shown. (C) Survival of $APS^{-/-}$ (closed circles) and wild-type (open circles) BMMCs by binding of monomeric IgE to FcεRI. Cells were cultivated in the absence or in the presence of various concentrations of monomeric IgE and percentages of live cells were measured. The average ± SD of three independent experiments are shown. (D) Tyrosine phosphorylation of total cellular proteins after cross-linking FcεRI. Sensitized BMMCs were stimulated with 2.5 μg/ml DNP-BSA for the indicated times. Total cell lysates were separated through SDS–PAGE and subjected to immunoblot using anti-phosphotyrosine mAb (4G10). Representative results of three experiments are shown.

Discussion

We investigated functions of Lnk, SH2-B or APS in mast cells, since possible regulatory roles of Lnk-family adaptor proteins in signaling through c-Kit or FcεRI had been suggested. We established BMMCs lacking either Lnk, SH2-B or APS and examined their cellular responses. None of those mutant BMMCs showed altered responses against IL-3 or SCF, the c-Kit ligand. *APS*-deficiency resulted in enhanced FcεRI-mediated degranulation, while both $lnk^{-/-}$ and $SH2\text{-}B^{-/-}$ BMMCs did not show any abnormal responses induced by cross-linking FcεRI.

We have shown that Lnk negatively regulates c-Kit signaling in B cell precursors and hematopoietic progenitor cells [8,10]. We did not observe significant enhancement in SCF-dependent growth of $lnk^{-/-}$ BMMCs in contrast to a previous report by Velazquez et al. [11]. SCF-dependent adherence was also comparable to normal cells. Expression levels of *lnk* transcripts are rather low in BMMCs compared to B-lineage cells or hematopoietic progenitor cells (unpublished data). It is likely that *lnk*-deficiency alone hardly affects mast cell function because of low expression of Lnk in mast cells.

APS had been cloned as a possible candidate substrate for the c-Kit [7]. However, $APS^{-/-}$ BMMCs did not show any altered responses upon stimulation with SCF. Instead, they showed enhanced FcεRI-mediated degranulation. $APS^{-/-}$ BMMCs showed reduced actin assembly at steady state compared to normal BMMCs. Inhibition of actin assembly in normal BMMCs by latrunculin resulted in enhanced degranulation similar to $APS^{-/-}$ BMMCs. In $APS^{-/-}$ mice, B-1 cells in peritoneal cavity increased and showed reduced F-actin contents. Conversely, in transgenic mice overexpressing APS in lymphocytes, B cells were reduced and showed enhanced actin assembly [17]. These results suggest that APS may negatively regulate degranulation process by controlling actin dynamics in mast cells. In RBL-2H3 mast cells, F-actin assembly induced by cross-linking FcεRI negatively controls degranulation as well as calcium signaling [22,23]. Oka et al. [24] recently reported that monomeric IgE binding induced actin assembly and that inhibition

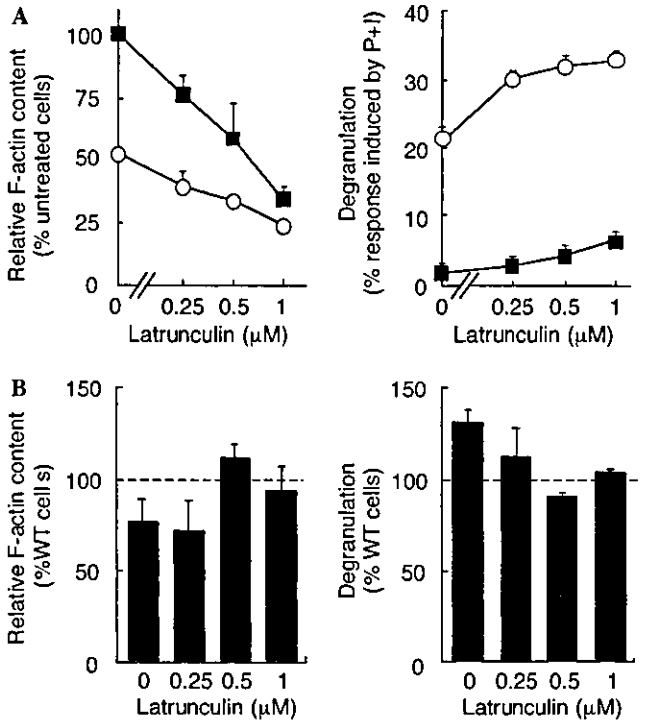

Fig. 4. Enhanced degranulation correlated with reduced F-actin contents in BMMCs treated with inhibitor of actin assembly, latrunculin or by APS-deficiency. (A) Treatment with latrunculin inhibited actin assembly and resulted in reduced F-actin content in BMMCs. Sensitized wild-type BMMCs were incubated with the various concentrations of latrunculin, kept unstimulated (squares) or stimulated with 2.5 μg/ml DNP-BSA (circles). F-actin contents of cells were then analyzed by rhodamine–phalloidin staining and flow cytometry, and the results are shown as relative F-actin contents compared with that of unstimulated cells in the absence of latrunculin (left). Degranulation was determined by measuring β-hexosaminidase activity released into culture supernatants, and results were shown as percent maximal responses induced by PMA and ionomycin treatment (right). (B) F-actin content of *APS*$^{-/-}$ BMMCs in the absence or the presence of various concentrations of latrunculin was measured and relative F-actin contents compared with those of control cells treated with the same concentrations of latrunculin were shown (left). Degranulation from *APS*$^{-/-}$ BMMCs treated with latrunculin was measured, and shown as percent reaction compared with those from wild-type control cells in the same conditions (right). Results shown are means ± SE of values obtained from three independent experiments.

of IgE-induced actin assembly by cytochalasin D initiates calcium influx and degranulation. Although enhancement of calcium influx in *APS*$^{-/-}$ BMMCs was not observed, reduction of actin assembly in *APS*$^{-/-}$ BMMCs may lead to augmented degranulation in analogy with those observed in RBL-2H3 mast cells. The molecular mechanisms for APS-mediated actin assembly as well as APS function downstream of cross-linking FcεRI remain to be elucidated.

APS function in insulin-R signaling has been also indicated in various experiments using cell lines [15,16,25–27]. *APS*$^{-/-}$ mice exhibited increased sensitivity to insulin and enhanced glucose tolerance [28]. It is intriguing to examine whether effect of *APS*-deficiency on insulin sensitivity is also mediated by actin dynamics. Regulation of actin cytoskeleton seems one of the common functions of Lnk-family adaptor proteins. Lnk associates with an actin binding protein ABP-280 [19] and facilitates actin assembly in overexpressed fibroblasts by activating Vav and Rac (S.M.K. and S.T., unpublished data). SH2-B is required for actin reorganization and regulates cell motility induced by GH-R activation [20,21].

SH2-B has been identified as a possible adaptor binding to ITAMs of FcεRI γ chain [6]. However, all examined responses induced by FcεRI ligation were normal with *SH2-B*$^{-/-}$ *BMMCs*. It seems *SH2-B*-deficiency do not affect mast cell function. However, it should be notified that interaction of SH2 domains of Lnk-family proteins with c-Kit or ITAM of FcεRI γ chain had been demonstrated in overexpression systems with different combinations, for example, SH2-B with FcεRI γ chain, APS with c-Kit. *SH2-B*$^{-/-}$ mice showed mild growth retardation and infertility due to impaired maturation of gonad organs [12]. Thus, SH2-B seemed to have a true target except FcεRI, worked as a positive regulator of signal transduction in contrast to Lnk and APS that function as negative regulators as shown in previous studies and in this study. Despite the significant structural similarities between APS, Lnk, and SH2-B, their functions appear to be quite different from each other. However, possible common functions of those adaptor proteins in vivo should be examined by generating mutant mice lacking APS, Lnk or SH2-B in various combinations.

In conclusion, our studies describe roles of Lnk family adaptor proteins on BMMCs. Both Lnk and SH2-B were dispensable for various mast cell responses mediated through c-Kit, FcεRI as well as IL-3-R. APS plays a role in controlling FcεRI-induced degranulation response but not in c-Kit-mediated proliferation or adhesion. APS may regulate degranulation by controlling actin dynamics in mast cells.

Acknowledgments

We thank our colleagues for helpful discussions, technical advices, and critical reading of the manuscript. This work was performed through Special Coordination Funds for Promoting Science and Technology, and Grants-in-Aid from the Ministry of Education, Culture, Sports, Science and Technology, the Japanese Government.

References

[1] D.D. Metcalfe, D. Baram, Y.A. Mekori, Mast cells, Physiol. Rev. 77 (1997) 1033–1079.
[2] S.J. Galli, Mast cells and basophils, Curr. Opin. Hematol. 7 (2000) 32–39.
[3] J. Rivera, Molecular adapters in Fc(epsilon)RI signaling and the allergic response, Curr. Opin. Immunol. 14 (2002) 688–693.

[4] J. Kalesnikoff, M. Huber, V. Lam, J.E. Damen, J. Zhang, R.P. Siraganian, G. Krystal, Monomeric IgE stimulates signaling pathways in mast cells that lead to cytokine production and cell survival, Immunity 14 (2001) 801–811.
[5] K. Vosseller, G. Stella, N.S. Yee, P. Besmer, c-kit receptor signaling through its phosphatidylinositide-3′-kinase-binding site and protein kinase C: role in mast cell enhancement of degranulation, adhesion, and membrane ruffling, Mol. Biol. Cell. 8 (1997) 909–922.
[6] M.A. Osborne, S. Dalton, J.P. Kochan, The yeast tribrid system: genetic detection of trans-phosphorylated ITAM-SH2-interactions, Biotechnology 13 (1995) 1474–1478.
[7] M. Yokouchi, R. Suzuki, M. Masuhara, S. Komiya, A. Inoue, A. Yoshimura, Cloning and characterization of APS, an adaptor molecule containing PH and SH2 domains that is tyrosine phosphorylated upon B-cell receptor stimulation, Oncogene 15 (1997) 7–15.
[8] S. Takaki, K. Sauer, B.M. Iritani, S. Chien, Y. Ebihara, K. Tsuji, K. Takatsu, R.M. Perlmutter, Control of B cell production by the adaptor protein Lnk: definition of a conserved family of signal-modulating proteins, Immunity 13 (2000) 599–609.
[9] M. Iseki, S. Takaki, K. Takatsu, Molecular cloning of the mouse APS as a member of the Lnk family adaptor proteins, Biochem. Biophys. Res. Commun. 272 (2000) 45–54.
[10] S. Takaki, H. Morita, Y. Tezuka, K. Takatsu, Enhanced hematopoiesis by hematopoietic progenitor cells lacking intracellular adaptor protein, Lnk, J. Exp. Med. 195 (2002) 151–160.
[11] L. Velazquez, A.M. Cheng, H.E. Fleming, C. Furlonger, S. Vesely, A. Bernstein, C.J. Paige, T. Pawson, Cytokine signaling and hematopoietic homeostasis are disrupted in Lnk-deficient mice, J. Exp. Med. 195 (2002) 1599–1611.
[12] S. Ohtsuka, S. Takaki, M. Iseki, K. Miyoshi, N. Nakagata, Y. Kataoka, N. Yoshida, K. Takatsu, A. Yoshimura, SH2-B is required for both male and female reproduction, Mol. Cell. Biol. 22 (2002) 3066–3077.
[13] M. Yokouchi, T. Wakioka, H. Sakamoto, H. Yasukawa, S. Ohtsuka, A. Sasaki, M. Ohtsubo, M. Valius, A. Inoue, S. Komiya, A. Yoshimura, APS, an adaptor protein containing PH and SH2 domains, is associated with the PDGF receptor and c-Cbl and inhibits PDGF-induced mitogenesis, Oncogene 18 (1999) 759–767.
[14] X. Qian, A. Riccio, Y. Zhang, D.D. Ginty, Identification and characterization of novel substrates of Trk receptors in developing neurons, Neuron 21 (1998) 1017–1029.
[15] Z. Ahmed, B.J. Smith, K. Kotani, P. Wilden, T.S. Pillay, APS, an adapter protein with a PH and SH2 domain, is a substrate for the insulin receptor kinase, Biochem. J. 341 (1999) 665–668.
[16] S.A. Moodie, J. Alleman-Sposeto, T.A. Gustafson, Identification of the APS protein as a novel insulin receptor substrate, J. Biol. Chem. 274 (1999) 11186–11193.
[17] M. Iseki, C. Kubo, S.M. Kwon, A. Yamaguchi, Y. Kataoka, N. Yoshida, K. Takatsu, S. Takaki, Increased numbers of B-1 cells and enhanced responses against TI-2 antigen in mice lacking APS, an adaptor molecule containing PH and SH2 domains, Mol. Cell. Biol. 24 (2004) in press.
[18] R. Setoguchi, T. Kinashi, H. Sagara, K. Hirosawa, K. Takatsu, Defective degranulation and calcium mobilization of bone-marrow derived mast cells from Xid and Btk-deficient mice, Immunol. Lett. 64 (1998) 109–118.
[19] X. He, Y. Li, J. Schembri-King, S. Jakes, J. Hayashi, Identification of actin binding protein, ABP-280, as a binding partner of human Lnk adaptor protein, Mol. Immunol. 37 (2000) 603–612.
[20] J. Herrington, M. Diakonova, L. Rui, D.R. Gunter, C. Carter-Su, SH2-B is required for growth hormone-induced actin reorganization, J. Biol. Chem. 275 (2000) 13126–13133.
[21] M. Diakonova, D.R. Gunter, J. Herrington, C. Carter-Su, SH2-Bβ is a Rac-binding protein that regulates cell motility, J. Biol. Chem. 277 (2002) 10669–10677.
[22] L. Frigeri, J.R. Apgar, The role of actin microfilaments in the down-regulation of the degranulation response in RBL-2H3 mast cells, J. Immunol. 162 (1999) 2243–2250.
[23] T. Oka, K. Sato, M. Hori, H. Ozaki, H. Karaki, Fc epsilonRI cross-linking-induced actin assembly mediates calcium signalling in RBL-2H3 mast cells, Br. J. Pharmacol. 136 (2002) 837–846.
[24] T. Oka, M. Hori, A. Tanaka, H. Matsuda, H. Karaki, H. Ozaki, IgE alone-induced actin assembly modifies calcium signaling and degranulation in RBL-2H3 mast cells, Am. J. Physiol. Cell Physiol. 17 (2003) 17.
[25] Z. Ahmed, B.J. Smith, T.S. Pillay, The APS adapter protein couples the insulin receptor to the phosphorylation of c-Cbl and facilitates ligand-stimulated ubiquitination of the insulin receptor, FEBS Lett. 475 (2000) 31–34.
[26] Z. Ahmed, T.S. Pillay, Functional effects of APS and SH2-B on insulin receptor signalling, Biochem. Soc. Trans. 29 (2001) 529–534.
[27] J. Liu, A. Kimura, C.A. Baumann, A.R. Saltiel, APS facilitates c-Cbl tyrosine phosphorylation and GLUT4 translocation in response to insulin in 3T3-L1 adipocytes, Mol. Cell. Biol. 22 (2002) 3599–3609.
[28] A. Minami, M. Iseki, K. Kishi, M. Wang, M. Ogura, N. Furukawa, S. Hayashi, M. Yamada, T. Obata, Y. Takeshita, Y. Nakaya, Y. Bando, K. Izumi, S.A. Moodie, F. Kajiura, M. Matsumoto, K. Takatsu, S. Takaki, Y. Ebina, Increased insulin sensitivity and hypoinsulinemia in APS knockout mice, Diabetes 52 (2003) 2657–2665.

The Role of IL-5 for Mature B-1 Cells in Homeostatic Proliferation, Cell Survival, and Ig Production[1]

Byoung-gon Moon,* Satoshi Takaki,* Kensuke Miyake,† and Kiyoshi Takatsu[2]*

B-1 cells, distinguishable from conventional B-2 cells by their cell surface marker, anatomical location, and self-replenishing activity, play an important role in innate immune responses. B-1 cells constitutively express the IL-5R α-chain (IL-5Rα) and give rise to Ab-producing cells in response to various stimuli, including IL-5 and LPS. Here we report that the IL-5/IL-5R system plays an important role in maintaining the number and the cell size as well as the functions of mature B-1 cells. The administration of anti-IL-5 mAb into wild-type mice, T cell-depleted mice, or mast cell-depleted mice resulted in reduction in the total number and cell size of B-1 cells to an extent similar to that of IL-5Rα-deficient (IL-5R$\alpha^{-/-}$) mice. Cell transfer experiments have demonstrated that B-1 cell survival in wild-type mice and homeostatic proliferation in recombination-activating gene 2-deficient mice are impaired in the absence of IL-5Rα. IL-5 stimulation of wild-type B-1 cells, but not IL-5R$\alpha^{-/-}$ B-1 cells, enhances CD40 expression and augments IgM and IgG production after stimulation with anti-CD40 mAb. Enhanced IgA production in feces induced by the oral administration of LPS was not observed in IL-5R$\alpha^{-/-}$ mice. Our results illuminate the role of IL-5 in the homeostatic proliferation and survival of mature B-1 cells and in IgA production in the mucosal tissues. *The Journal of Immunology,* **2004, 172: 6020–6029.**

B-1 cells differ from conventional B-2 cells in their surface phenotype, anatomical localization, self-replenishing activity, and V_H usage of IgM (1, 2). B-1 cells constitutively express three different markers, namely Mac-1 (CD11b/CD18), FcεR (CD23), and the IL-5R α-chain (IL-5Rα).[3] Mac-1 is present in peritoneal and pleural cavity B-1 cells but is not expressed on B-2 cells, whereas FcεR is preferentially expressed on B-2 cells in the peritoneal cavity and in the spleen (3, 4). IL-5Rα is constitutively expressed on all B-1 cells, but is expressed on a small proportion (2–4%) of resting B-2 cells in the spleen (5).

The progenitors of B-1 cells are abundant in the fetal omentum and liver but are missing in the bone morrow of adult animals (6, 7). In contrast with B-2 cells, which are supplied from progenitors in the bone marrow throughout life, B-1 cells maintain their number in adult animals by their self-replenishing capacity (3, 7). In the adult, these self-replenishing B-1 cells are clearly enriched in the peritoneal and pleural cavities, and a low frequency is seen in the spleen, but B-1 cells are virtually absent from the lymph nodes, Peyer's patches (PP), and peripheral blood, where most conventional B-2 cells are localized (3). B-1 cells are categorized into B-1a cells that express CD5 and B-1b cells that express cell surface markers similar to those of B-1a cells, except for the low expression, if any, of CD5 (2, 3).

B-1 cells are believed to be the primary source of natural IgM Ab, although they can become Ig-producing cells for all isotypes. Consistent with a major role of B-1 cells in natural IgM production, a number of specificities of natural IgM Ab have been identified in the B-1 repertoire. These include specificities for LPS, phosphorylcholine, undefined determinants on *Escherichia coli* and *Salmonella* spp., phosphatidylcholine, and complement-binding Abs (3). Furthermore, B-1 cells in the peritoneal cavity serve as an important source of IgA-producing plasma cells at mucosal sites. These findings are largely supported by transfer experiments of peritoneal B-1 cells in irradiated mice or otherwise B cell-depleted mice and by analysis of genetically altered immune-deficient mice (8). The role of B-1 cells in IgA production in the gut is further supported by evidence that mice with a selective B-1 cell reduction in number showed decreased frequencies of IgA-producing cells in the lamina propria (LP) (9). The helper T cell dependency of B-1 cells on gut-associated IgA production is still controversial (9, 10).

Studies of gene-targeted and transgenic mice have revealed that B cell receptor (BCR) signaling is critical for B-1 cell development or maintenance. Mutant mice that lack Bruton's tyrosine kinase protein kinase C β, CD19, the p85α subunit of phosphatidylinositol-3 kinase, p95^{vav}, CD21/CD35, and CD81, which are strongly associated with BCR signaling, have substantial depletion of B-1 cells but largely spare B-2 cells (11–18). Conversely, mutation or overexpression of Src homology protein-1, CD22, or CD72 that induces enhanced BCR signaling results in an expanded B-1 cell compartment (19–21).

IL-5, mainly produced by activated Th2 cells and mast cells, acts on B-1 and B-2 cells to induce proliferation and differentiation into Ig-producing cells (22–25). IL-5 also controls the production and functions of eosinophils and basophils. The IL-5R consists of two distinct membrane proteins, IL-5Rα and βc, each of which is a member of the cytokine receptor superfamily (5). The binding of IL-5 occurs through the IL-5Rα, and the βc forms a high-affinity IL-5R in combination with the IL-5Rα, transducing signals into nuclei. Although the molecular mechanisms for IL-5 signal

Divisions of *Immunology and †Infectious Genetics, Department of Microbiology and Immunology, Institute of Medical Science, University of Tokyo, Tokyo, Japan

Received for publication October 30, 2003. Accepted for publication March 3, 2004.

The costs of publication of this article were defrayed in part by the payment of page charges. This article must therefore be hereby marked *advertisement* in accordance with 18 U.S.C. Section 1734 solely to indicate this fact.

[1] This work was supported by a research grant from the Human Frontier Science Program (to K.T.), by Special Coordination Funds for Promoting Science and Technology (to K.T.), by a Grant-in-Aid for Scientific Research on Priority Areas from the Ministry of Education, Science, Sports and Culture (Japan), and by an international postdoctoral fellowship from the Japan Society for the Promotion of Science (to B.M.).

[2] Address correspondence and reprint requests to Dr. Kiyoshi Takatsu, Division of Immunology, Department of Microbiology and Immunology, Institute of Medical Science, University of Tokyo, 4-6-1 Shirokanedai Minato-ku, Tokyo 108-8639, Japan. E-mail address: takatsuk@ims.u-tokyo.ac.jp

[3] Abbreviations used in this paper: IL-5Rα, IL-5R α-chain; PP, Peyer's patch; LP, lamina propria; BCR, B cell receptor; RAG, recombination-activating gene; PEC, peritoneal exudate cell; MLN, mesenteric lymph node; s, surface; TLR, Toll-like receptor 4; HPRT, hypoxanthine phosphoribosyltransferase; m, murine; CD40L, CD40 ligand.

0022-1767/04/$02.00

transduction are not fully characterized, the activation of Bruton's tyrosine kinase and Janus kinase 2 kinases, rapid tyrosine phosphorylation of βc and Src homology 2/Src homology 3-containing cellular proteins, and the induction of the transcription of several nuclear proto-oncogenes are essential for signal transduction (26–32).

Transgenic mice expressing the *IL-5* gene exhibit elevated levels of serum IgM, IgA, and IgE, and an increase in the number of B-1 cells and autoantibody production and show persistent eosinophilia (33, 34). IL-5Rα$^{-/-}$ mice and IL-5$^{-/-}$ mice show a decrease in B-1 cells in the peritoneal cavity and in B-1 cell-derived surface (s)IgA^{+} cells in the LP (35–39). Although these results suggest that IL-5 is an important cytokine for B-1 cell development, maintenance, or triggering, the role of IL-5 in mature B-1 cell maintenance and activation in vivo remains to be properly evaluated.

This study examines whether the IL-5/IL-5R system plays an important role in the homeostatic proliferation and survival of mature B-1 cells. We show that IL-5 regulates the cell number and cell size of B-1 cells in the absence of T cells or mast cells. We also demonstrate the role of IL-5 in gut-associated B-1 cell response to CD40 and LPS.

Materials and Methods

Mice

C57BL/6J (IL-5Rα$^{+/+}$) and W/W^{V} mice were purchased from Japan SLC (Hamamatsu, Japan). Recombination-activating gene (RAG)2-deficient (RAG-2$^{-/-}$) mice and TCRβ δ double null mutant (TCRβ$^{-/-}$ δ$^{-/-}$) mice were purchased from The Jackson Laboratory (Bar Harbor, ME). The IL-5Rα null mutant (IL-5Rα$^{-/-}$) mice (35) used in this study were backcrossed with C57BL/6J mice for >10 generations. IL-5 null mutant (IL-5$^{-/-}$) mice on a C57BL/6 background (38) were donated by M. Kopf (University of Freiburg, Germany). All of the mice were bred and maintained in animal facilities under specific pathogen-free conditions using ventilated microisolater cages in the experimental animal facility at the Institute of Medical Science, University of Tokyo. All experiments were conducted according to our institution's guidelines for the care and treatment of experimental animals.

Administration of anti-IL-5 mAb and LPS

A single i.p. administration of anti-IL-5 mAb (clone NC17) or isotype-matched control IgG into 6- to 8-wk-old mice (1 mg in a volume of 250 μl per mouse) was performed (40, 41). Six days after treatment, peritoneal washouts were obtained and analyzed. LPS (*E. coli* serotype O55: B5; Sigma-Aldrich, St. Louis, MO) dissolved in PBS was orally administered (0.1 mg in a volume of 200 μl per mouse per week) for 3 wk into the gut of 8-wk-old mice through a 1-mm diameter polyethylene tube. Seven days after the last administration, the mice were anesthetized with ether, sacrificed, and analyzed.

Cell preparation

Single cell suspensions were prepared from the lymphoid organs of 6- to 8-wk-old mice. A standard procedure was used to prepare single cell suspensions from the peritoneal exudate cells (PECs), mesenteric lymph nodes (MLNs), PP, SP, lung, and the LP of the small intestine. Briefly, PECs were obtained by washing the peritoneal cavity with HBSS (Life Technologies, Grand Island, NY) containing 3% FCS. Mononuclear cells from MLNs or PP were isolated by a mechanical method using a stainless steel screen. Mononuclear cells from the lung and LP were isolated by a procedure of shaking in an RPMI 1640 medium (Life Technologies) containing 5 mM EDTA and by enzymatic dissociation procedures with collagenase type VIII (Sigma-Aldrich) (37).

Purification of B-1 cells

PECs were collected from >10 mice and were mixed together. After washing twice with PBS containing 1% BSA, the cells were incubated with anti-FcγR (2.4G2; American Type Culture Collection, Rockville, MD) to prevent the nonspecific binding of the labeled Abs. After another washing, macrophages, B-2 cells, and T cells were depleted from the cells using a MACS system (Miltenyi Biotec, Cologne, Germany) after incubation with a mixture of biotinylated Abs (anti-F4/80, anti-CD23, and anti-CD3) and streptavidine-coupled microbeads (Miltenyi Biotec). In B-1 cell transfer experiments, we took another purification step of B-1 cells using a FACSVantage (BD Biosciences, San Jose, CA) to obtain B-1 cells with a higher degree of purity. In addition to using the MACS system, the resulting F4/80^{-}/CD23^{-}/CD3^{-} cells were stained with FITC-labeled anti-CD23 and PE-labeled F(ab')$_2$ of anti-IgM, and the CD23^{-}sIgM^{+} cells were sorted using a FACSVantage.

Flow cytometry

The cells (1–10 × 10^5) were stained with predetermined optimal concentrations of the respective Abs together with 2.4G2 (10 μg/ml). After washing, the cells were analyzed on FACScan or a FACSCaliber instrument (BD Biosciences). The following mAbs were used: biotinylated anti-IL-5Rα (T21) (42); FITC-labeled, PE-labeled, or biotinylated anti-CD23 (B3B4), PE-labeled or biotinylated anti-CD5 (53-7.3) and biotinylated anti-CD3 (145-2C11) (all purchased from BD PharMingen, San Diego, CA); FITC-labeled, PE-labeled, or biotinylated anti-B220 (RA3-6B2), PE-labeled F(ab')$_2$ of anti-mouse IgM, and FITC-labeled or biotinylated anti-Mac-1 (M1/70) (all obtained from Caltag Laboratories, Burlingame, CA); PE-labeled anti-Toll-like receptor 4 (TLR4)/MD2 (MTS 510) (43) and PE-labeled anti-RP105 (RP/14) (44); biotinylated anti-CD40 (1C10; R&D Systems, Minneapolis, MN), biotinylated anti-F4/80 (A3-1; Serotec, Oxford, U.K.); and biotinylated anti-IgA (Southern Biotechnology, Birmingham, AL). PE-labeled streptavidin (Ancell, Bayport, MN) or allophycocyanin-conjugated streptavidine (BD PharMingen) were also used. In some stainings, 2 μg/ml 7-amino-actinomycin D (Sigma-Aldrich) was used to gate out dead cells.

Cell transfer and homeostatic proliferation assay

PECs obtained from IL-5Rα$^{+/+}$ or IL-5Rα$^{-/-}$ mice were washed with PBS and suspended in PBS at 1 × 10^7 cells/ml. CFSE (Molecular Probes, Eugene, OR) was then added to the cell suspensions at a final concentration of 1 μM. The cell suspensions were incubated at 37°C for 10 min and washed three times with cold sterile PBS. The resulting CFSE-labeled cells (1 × 10^6) were injected i.p. into IL-5Rα$^{+/+}$ or RAG-2$^{-/-}$ mice. In some experiments, sorted B-1 cells (1 × 10^5) were injected i.p. into RAG-2$^{-/-}$ mice. The PECs of recipient mice were recovered on days 2, 30, and 60 after the cell transfer, and their cellularities in the B-1 cell compartment were analyzed.

RNA isolation and semiquantitative RT-PCR

Total RNA was isolated from various mouse tissues using the SV Total RNA Isolation System (Promega, Madison, WI), according to the manufacturer's instructions, and first strand cDNA templates synthesized by Superscript II reverse transcriptase (Life Technologies) using random primers (TaKaRa, Kyoto, Japan). Serial dilutions of cDNA templates were subjected to PCR amplification by using primer sets encompassing several introns for IL-5 (forward primer, 5'-ATGGAGATTCCCATGAGCAC; reverse primer, 5'-GCACAGTTTTGTGGGGTTTT) or hypoxanthine phosphoribosyltransferase (HPRT; forward primer, 5'-TGCTCGAGATGTCATGAAGG; reverse primer, 5'-TTGCGCTCATCTTAGGCTTT). The cycling parameters were 1 min at 94°C, 1 min at 60°C, and 1 min at 72°C for 35 cycles to detect *IL-5* mRNA or 27 cycles for HPRT. The PCR products were separated through 1.0% agarose gel and were stained with ethidium bromide.

Assay for B-1 cell proliferation and differentiation

MACS-sorted PECs were cultured in an RPMI 1640 medium supplemented with 8% heat-inactivated FCS, 2 mM glutamine, 5 μM 2-ME, penicillin (100 U/ml), and streptomycin (100 μg/ml) in 96-well flat-bottom microtiter plates (1 × 10^5/well in 200 μl of medium) with or without stimulants. Anti-CD40 mAb (1C10; R&D Systems; 1 μg/ml), LPS (40 μg/ml), IL-4 (1000 U/ml), or a selected combination of these agents was added at the onset of cell culture. For the proliferation assay, cells were pulse-labeled with [^{3}H]thymidine (0.2 μCi per well) during the last 8 h of the 72-h culture period, and the incorporated [^{3}H]thymidine was measured using a MATRIX 96 Direct Beta Counter (Packard, Meriden, CT). The results were expressed as the mean cpm and the SD of the duplicate cultures. For determining IgM, IgG1, and IgG3 secretion, cells (1 × 10^5 in a 200-μl culture) were cultured for 7 days. The cultured supernatants were used for ELISA to determine the amounts of IgM, IgG1, and IgG3. Each experiment was repeated at least three times.

Enumeration of Ig-producing cells using ELISPOT

An ELISPOT assay was conducted according to the procedures previously described (37). The 96-well filtration plates with a nitrocellulose base (Millipore, Bedford, MA) were coated with 5 μg/ml anti-Ig (Southern Biotechnology) overnight and were blocked with a culture medium. The mononuclear cells suspended in the culture medium were added at various concentrations and were incubated for 6 h. After washing, 1 μg/ml HRP-conjugated anti-IgM, anti-IgG, or anti-IgA Ab (all obtained from Southern Biotechnology) was added, and the plates were incubated for 10 h at 4°C.

After the incubation, the spots were developed with 2-amino-9-ethylcarbazole containing hydrogen peroxide (Polysciences, Warrington, PA). Reddish-brown-colored spots were counted as Ab-forming cells using the KS ELISPOT compact system (Carl Zeiss, Jena, Germany).

ELISA

Freshly collected fecal samples were weighed, dissolved in PBS (0.1 g/ml), and centrifuged at 15,000 rpm for 5 min. The supernatants were used as fecal extract. The amount of each Ig isotype in sera and in fecal extract was measured by sandwich ELISA with Abs specific for each murine (m)Ig isotype according to the procedures previously described (36). In brief, 96-well trays (Greiner, Frickenhausen, Germany) were coated with 10 μg/ml isotype-specific goat anti-mIg polyclonal Abs for total Igs. Samples were added to the wells and the trays were incubated for 2 h. After washing with PBS containing 0.05% Tween 20 (washing buffer), biotinylated isotype-specific goat anti-mIg polyclonal Abs were added to each well. After washing, HRP-streptavidine was added to each well, and the incubation continued for 1 h. Finally, the trays were washed with the buffer, and 100-μl aliquots of substrate, *o*-phenylene-diamine (final 0.4 mg/ml), and hydrogen peroxide (final 0.015%), dissolved in 0.1 M citrate buffer (pH 5.0), were added to each well. Enzyme reaction was terminated by adding 2 M sulfuric acid, and OD at 495 nm was measured with a V-max kinetic Micro Plate Reader (Molecular Devices, Sunnyvale, CA). Using myeloma proteins (BD PharMingen), standard curves were generated for each isotype and the concentration of mIg was determined.

Results

Decrease in cell number and cell size of mature B-1 cells by administration of anti-IL-5 mAb in vivo

As we reported previously, IL-5Rα$^{-/-}$ mice have a significant reduction in cell number and cell size of IgM$^+$ CD5$^+$ B-1a cells in the PECs (36). When we analyzed the entire IgM$^+$ CD23$^-$ B-1 cell populations, a significant reduction in percentage and smaller cell size of B-1 cells was also observed (Fig. 1*A*). These results were confirmed by the analysis of IgM$^+$ CD5$^+$ B-1 cell populations. We also found that the total number and size of B-1 cells in the PECs decreased in IL-5$^{-/-}$ mice (data not shown). In contrast with B-1 cells, the total percentage and size of IgM$^+$CD23$^+$ (or IgM^{low}CD5$^-$) B-2 cells in IL-5Rα$^{-/-}$ mice were similar to those of wild-type mice (Fig. 1*A*). The total numbers of B-1 cells in IL-5Rα$^{+/+}$ and IL-5Rα$^{-/-}$ mice were 4.2×10^5 and 3.1×10^5 on average, respectively, (statistically significant, $p < 0.05$), whereas those of B-2 cells were 4.0×10^5 and 4.3×10^5, respectively (Table I).

Our first question is whether the abnormalities observed in B-1 cells from IL-5Rα$^{-/-}$ and IL-5$^{-/-}$ mice originated in the developmental process or in fully developed mature B-1 cells. We administered anti-IL-5 mAb i.p. into a group of 8-wk-old wild-type mice, which developed mature B-1 cells. As a control, isotype-matched rat IgG was injected in another group of mice. A smaller B-1 cell size was observed in anti-IL-5-treated mice 3 days after treatment (data not shown). Six days after anti-IL-5 treatment, not only cell size but also the total percentage of B-1 cells significantly decreased (Fig. 1*B*). The total numbers of B-1 cells on average in the control and anti-IL-5-treated mice were 4×10^5 and 3.2×10^5, respectively (statistically significant, $p < 0.05$), whereas those of B-2 cells were 3.8×10^5 and 3.7×10^5, respectively (Table I). The levels of reduction in B-1 cell number and size in anti-IL-5-treated mice were similar to those of B-1 cells in IL-5Rα$^{-/-}$ mice. Anti-IL-5 treatment did not cause significant changes in total number or cell size in the IgM$^+$CD23$^+$ (or IgM^{low}CD5$^-$) B-2 cell compartment (Fig. 1*B*). We infer from these results that the abnormality of B-1 cells observed in IL-5Rα$^{-/-}$ mice is reproduced in mature B-1 cells in wild-type mice by blocking IL-5 signals.

Impaired survival and homeostatic proliferation of B-1 cells in IL-5Rα$^{-/-}$ mice

To examine the role of IL-5 in maintaining the mature B-1 cell compartment in more detail, PECs from IL-5Rα$^{+/+}$ or IL-5Rα$^{-/-}$ mice were labeled with CFSE and transferred into the peritoneal cavity of unirradiated IL-5Rα$^{+/+}$ mice, where the normal number

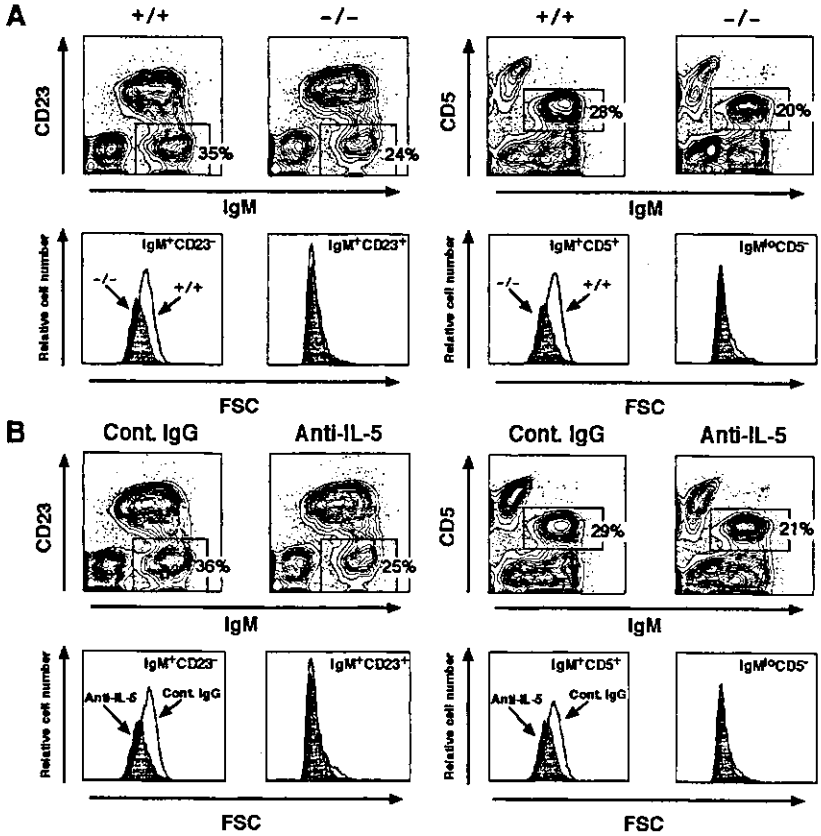

FIGURE 1. Decreased cell number and size of B-1 cells by blocking IL-5 and IL-5R interaction. Representative two-color contour plots show the expression of IgM/CD23 and IgM/CD5 on PECs from 8-wk-old IL-5Rα$^{+/+}$ or IL-5Rα$^{-/-}$ mice (*A*) and from control IgG- or anti-IL-5-treated IL-5Rα$^{+/+}$ mice (*B*). A single i.p. administration of anti-IL-5 mAbs or control IgG (1 mg/250 μl) into IL-5Rα$^{+/+}$ mice was performed. PECs were obtained and analyzed on day 6 after treatment (*B*). The percentages represent the fractions of the lymphocyte-gated live cells that fall into the indicated boxes. Representative histograms depict the relative cell number and sizes of B-1 cells (IgM$^+$CD23$^-$), B-1a cells (IgM$^+$CD5$^+$), and B-2 cells (IgM$^+$CD23$^+$ or IgM^{low}CD5$^-$). The representative results of three independent experiments are shown.

Table I. *Reduced absolute cell number of B-1 cells by blocking IL-5 and IL-5R interaction*[a]

	IL-5Rα$^{+/+}$	IL-5Rα$^{-/-}$	Control IgG	Anti-IL-5
B-1 (IgM$^+$CD23$^-$)	4.2 ± 0.36	3.1 ± 0.34*	4.4 ± 0.32	3.2 ± 0.17*
B-1a (IgM$^+$CD5$^+$)	3.8 ± 0.28	2.8 ± 0.39*	4.0 ± 0.41	3.0 ± 0.23*
B-2 (IgM$^+$CD23$^+$)	4.0 ± 0.42	4.3 ± 0.52	3.8 ± 0.21	3.7 ± 0.33

[a] The results indicate the mean cell numbers ± SEM (× 10^5) of indicated groups of five mice.
*, $p < 0.05$ compared with IL-5Rα$^{+/+}$ or control IgG-administered mice.

of B-1 cells resides. The CFSE$^+$ B-1 and CFSE$^+$ B-2 cells in the PECs of the recipient mice were examined by FACS analysis on day 2 or on day 30. As shown in Fig. 2*A* (*left panel*), the proportion of CFSE$^+$IL-5Rα$^{+/+}$ B-1 cells on day 30 (94%) was close to that on day 2, suggesting the long-term survival of CFSE-labeled B-1 cells in the recipient. In contrast, the proportion of CFSE$^+$ IL-5Rα$^{-/-}$ B-1 cells was reduced to 39% on day 30 compared with that on day 2. The intensity of CFSE labeling showed a broad distribution in both IL-5Rα$^{+/+}$ B-1 and IL-5Rα$^{-/-}$ B-1 cells on day 30 (Fig. 2*B*), indicating that cells have divided slightly. However, we could not estimate how many times the B-1 cells divided, because of faint intensities of CFSE labeling. CFSE$^+$ IL-5Rα$^{+/+}$ B-2 cells in the recipient on day 30 were reduced to 55%, which was comparable with CFSE$^+$IL-5Rα$^{-/-}$ B-2 cells (52%) (Fig. 2*A*, *right panel*). We examined the distribution of CFSE-positive B cells from IL-5Rα$^{+/+}$ or IL-5Rα$^{-/-}$ mice in the LP, PP, and MLNs of recipient mice 30 days after cell transfer. CFSE-positive B cells were rarely detected in the LP (data not shown). We observed some CFSE-positive B cells (0.02–0.03% of the total cells) in MLNs and PP (data not shown). However, there was no significant difference between recipient mice transferred IL-5Rα$^{+/+}$B-1 and IL-5Rα$^{-/-}$B-1 cells. Thus, the survival of mature B-1 cells, but not B-2 cells, in the peritoneal cavity was severely impaired in the absence of IL-5Rα.

Next, the role of IL-5 in the self-replenishing activity of B-1 cells was examined. Peritoneal exudate cells from IL-5Rα$^{+/+}$ or IL-5Rα$^{-/-}$ mice were CFSE-labeled and transferred into RAG-2$^{-/-}$ mice. On day 30, the proportion of CFSE$^+$ IL-5Rα$^{+/+}$ B-1 cells in the recipient RAG-2$^{-/-}$ mice increased ~3-fold (276%) compared with that on day 2, whereas the proportion of CFSE$^+$ IL-5Rα$^{-/-}$ B-1 cells did not increase (70%) (Fig. 3*A*, *upper panel*). The CFSE intensity of IL-5Rα$^{-/-}$ B-1 cells somewhat decreased, but maintained higher intensities than did IL-5Rα$^{+/+}$ B-1 cells (Fig. 3*B*, *lower left panel*). The difference in B-2 cell number on day 30 in the RAG-2$^{-/-}$ recipient mice between IL-5Rα$^{+/+}$ B-2 cells and IL-5Rα$^{-/-}$ B-2 cells (62% and 48%, respectively) was not obvious compared with that of B-1 cells (Fig. 3*A*, *lower panel*). The CFSE intensity of IL-5Rα$^{-/-}$ B-2 cells was comparable with that of IL-5Rα$^{+/+}$ B-2 cells (Fig. 3*B*, *lower right panel*). In the LP 30 days after cell transfer, the proportion of CFSE$^+$B220$^-$sIgA$^+$ cells in RAG-2$^{-/-}$ mice transferred with IL-5Rα$^{+/+}$ cells was significantly higher than that transferred with IL-5Rα$^{-/-}$ cells (Fig. 3*C*, *left panels*). We examined the levels of CFSE in sIgA$^+$ cells in the LP in recipients transferred IL-5Rα$^{+/+}$ PECs or IL-5Rα$^{-/-}$ PECs and found that the levels of CFSE of sIgA$^+$ cells were very low and were similar between the two experimental groups (Fig. 3*C*, *right panels*). Intriguingly, ~3-fold higher levels of IgM, IgG1, IgG3, and IgA in serum were observed in RAG-2$^{-/-}$ mice transferred IL-5Rα$^{+/+}$ cells compared with those transferred with IL-5Rα$^{-/-}$ cells, whereas the serum levels of IgG2a and IgG2b were comparable between the two groups (Fig. 3*D*, *left panel*). The amount of IgA in fecal extracts was also ~3-fold higher in the recipients of IL-5Rα$^{+/+}$ cells compared with that in IL-5Rα$^{-/-}$ cells (Fig. 3*D*, *right panel*). These results imply that IL-5 plays a critical role in the homeostatic proliferation of mature B-1 cells and leads to the maintenance of optimal levels of Ig production, although these processes may occur inefficiently even in the absence of IL-5.

Homeostatic proliferation and Ig production of B-1 cells in the absence of T cells

We examined the effect of T cell dependency in the IL-5-mediated homeostatic proliferation of mature B-1 cells. IgM$^+$CD23$^-$ B-1 cells were purified (>98% purity) from the PECs of IL-5Rα$^{+/+}$ or IL-5Rα$^{-/-}$ mice by cell sorting and were transferred into RAG-2$^{-/-}$ mice. As shown in Fig. 4*A*, the proportion of IL-5Rα$^{+/+}$ B-1 cells in PECs increased ~2-fold (198%) on day 30 and ~3-fold (276%) on day 60 in the RAG-2$^{-/-}$ recipient mice. An increase in both the IgM$^+$CD23$^-$CD5$^+$B-1a and IgM$^+$CD23$^-$CD5$^-$B-1b cell populations was also observed (Fig. 4*A*, *center* and *right*

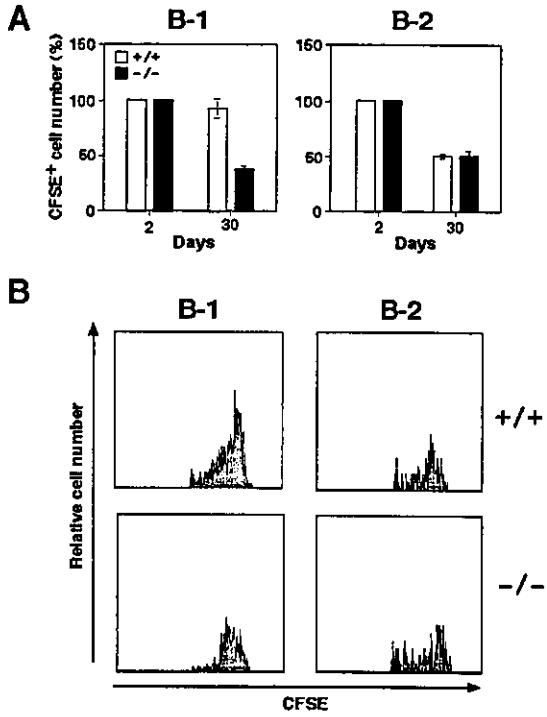

FIGURE 2. Impaired survival of mature IL-5Rα$^{-/-}$ B-1 cells. CFSE-labeled PECs from IL-5Rα$^{+/+}$ or IL-5Rα$^{-/-}$ mice were transferred (1 × 10^6 cells per head) into the peritoneal cavity of IL-5Rα$^{+/+}$ mice. On days 2 and 30 after cell transfer, the recipient mice were killed and the numbers of CFSE$^+$ B-1 (IgM$^+$CD23$^-$) and B-2 (IgM$^+$CD23$^+$) cells in PECs were analyzed by flow cytometry. Two and three recipient mice in each group were analyzed and the mean ± SEM is shown (*A*). The mean cell number of CFSE$^+$ peritoneal cells from two mice on day 2 was set as 100% (*A*). Representative histograms show the intensity of CFSE in B-1 cells (CFSE$^+$IgM$^+$CD23$^-$) and B-2 cells (CFSE$^+$IgM$^+$CD23$^+$) in the peritoneal cavity of the recipients (*B*). The data shown are representative results from three independent experiments.

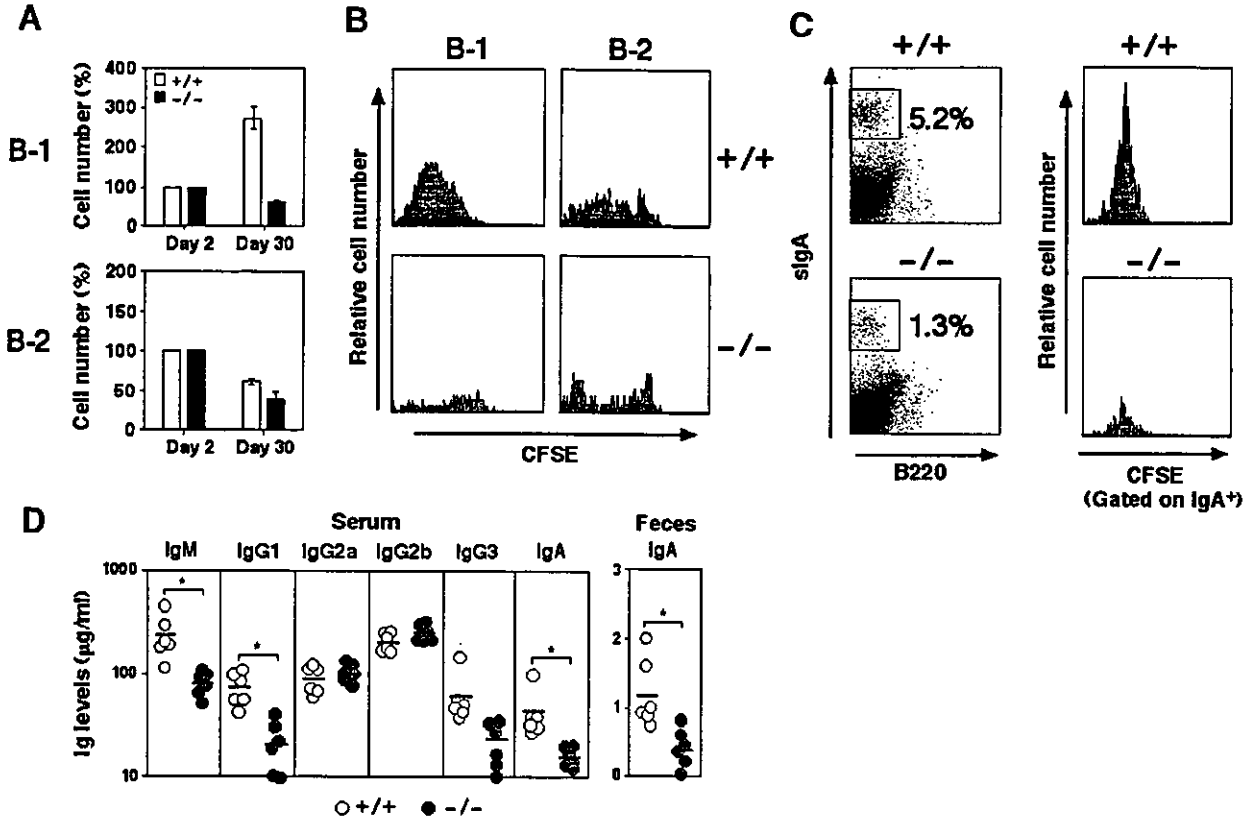

FIGURE 3. Impaired homeostatic B-1 cell proliferation and Ig production from IL-5R$\alpha^{-/-}$ mice. *A*, IL-5R$\alpha^{-/-}$ B-1 cells have a defect in homeostatic proliferation. CFSE-labeled peritoneal cells were injected i.p. into RAG-$2^{-/-}$ mice. The recipient mice of each group were analyzed as described in Fig. 2. *B*, IL-5R$\alpha^{-/-}$ B-1 cells maintain high CFSE intensity. Representative histograms depict CFSE intensity in B-1 cells and B-2 cells in PECs of RAG-$2^{-/-}$ recipient mice. *C*, IL-5R$\alpha^{-/-}$ B-1 cells migrate to the LP, but the number of sIgA$^+$ cells is decreased. Cells in the LP were purified as in the method described and were stained with anti-B220 and anti-IgA. Representative two-color fluorescence plots show B220$^+$ and sIgA$^+$ cells in the LP of the recipient mice on day 30. Representative histograms depict CFSE intensity in sIgA$^+$ cells in LP of RAG-$2^{-/-}$ recipient mice. The percentages represent the fractions of the lymphocyte gated live cells that fall into the indicated box. Representative results of three independent experiments are shown (*A–C*). *D*, IL-5R$\alpha^{-/-}$ peritoneal cells transferred into RAG-$2^{-/-}$ mice produce low levels of Igs. The concentration of Ig subclasses in serum or in fecal extracts in the RAG-$2^{-/-}$ recipient mice on day 30 was determined by isotype-specific ELISA. The mean values of Igs in the indicated groups of recipient mice are represented as a bar. *, $p < 0.05$ by Student's *t* test.

panels), whereas CD5^{high} T cells or CD23$^+$ B-2 cells were not detected even 60 days after cell transfer (data not shown). In contrast, IL-5R$\alpha^{-/-}$ B-1 cells did not show a significant increase on day 30 (114%) or on day 60 (103%) compared with that 2 days after cell transfer (Fig. 4*A*, *left panel*). IL-5R$\alpha^{-/-}$ B-1a cells decreased to ~71% on day 30 and on day 60, whereas IL-5R$\alpha^{-/-}$ B-1b cells showed a small but significant increase up to 129% on day 30 (Fig. 4*A*, *center* and *right panels*). These results indicate that mature B-1 cells undergo homeostatic proliferation in T cell-deficient conditions. The serum levels of IgM, IgG3, and IgA were elevated to ~3- to 5-fold in the recipient transferred IL-5R$\alpha^{+/+}$ B-1 cells compared with those of IL-5R$\alpha^{-/-}$ B-1 cells (Fig. 4*B*). The Ig levels of IgG1 and IgG2 were virtually undetectable in both groups of recipient mice on day 30 (Fig. 4*B* and data not shown).

Production of IL-5 in T cell- and mast cell-deficient mice

IL-5 is produced by T cells, mast cells, and eosinophils once they are activated (22). In particular, not only $\alpha\beta$T cells in the peritoneal cavity and intestinal intraepithelial lymphocytes (8, 45), but also freshly isolated $\gamma\delta$T cells in the intraepithelial lymphocytes are capable of producing IL-5 (45). We injected anti-IL-5 mAb into TCR$\beta^{-/-}\delta^{-/-}$ mice and examined B-1 cell survival in T cell-deficient conditions. Anti-IL-5-treated TCR$\beta^{-/-}\delta^{-/-}$ mice showed a decrease in B-1 cell number and cell size 6 days after treatment, compared with the control group of mice (Fig. 5*A*, *left panel*). Anti-IL-5 injection into W/W^V mice also caused a decrease in B-1 cell size (Fig. 5*A*, *right panel*), although the total B-1 cell number did not change significantly. The total number and size of B-2 cells did not change in either the TCR$\beta^{-/-}\delta^{-/-}$ mice or the W/W^V mice as a result of anti-IL-5 treatment (data not shown).

To evaluate *IL-5* mRNA expression in tissues, total RNA was isolated from the various tissues of RAG-$2^{-/-}$, TCR$\beta^{-/-}\delta^{-/-}$, and W/W^V mice and was used for *IL-5* mRNA expression analysis. As controls, wild-type mice and IL-$5^{-/-}$ mice were also used. RT-PCR analysis revealed significant *IL-5* mRNA expression in the lungs, spleen, small intestine, and stomach of wild-type mice, RAG-$2^{-/-}$ mice, TCR$\beta^{-/-}\delta^{-/-}$, and W/W^V mice (Fig. 5*B*). A lesser extent of *IL-5* mRNA expression was observed in PECs. We did not detect any *IL-5* mRNA expression in the tissues of the IL-$5^{-/-}$ mice. *IL-5* mRNA expression was not observed in the liver. To examine *IL-5* mRNA expression in cells other than T cells, mast cells, and eosinophils, we purified c-*kit*$^-$IL-5Rα^- cells by sorting (>99% purity) from the tissues of RAG-$2^{-/-}$ mice. The RNA from these cells was isolated and used for RT-PCR analysis. As shown in Fig. 5*C*, high levels of *IL-5* mRNA expression were observed in c-*kit*$^-$IL-5Rα^- cells in the lungs and small intestine of RAG-$2^{-/-}$ mice. The c-*kit*$^-$IL-5Rα^- PECs also expressed *IL-5* mRNA, although the expression levels were low. These results

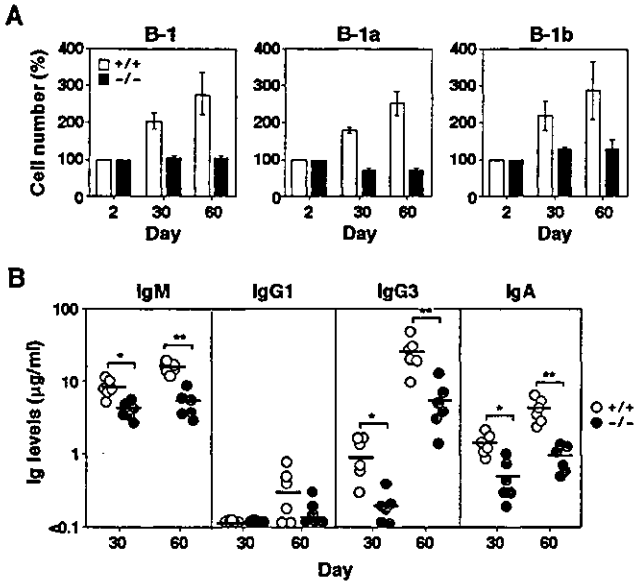

FIGURE 4. T cell-independent homeostatic proliferation of B-1 cells. *A*, B-1 cells from IL-5Rα$^{+/+}$ mice but not from IL-5Rα$^{-/-}$ mice show homeostatic proliferation even in T cell-deficient conditions. Purified B-1 cells were transferred (1×10^5 per head) i.p. into RAG-2$^{-/-}$ mice. The proportion of B-1 (IgM$^+$CD23$^-$), B-1a (IgM$^+$CD23$^-$CD5$^+$), or B-1b (IgM$^+$CD23$^-$CD5$^-$) cells in the PECs of RAG-2$^{-/-}$ mice was analyzed by flow cytometry. The recipient mice of each group were analyzed as described in Fig. 2 on days 2, 30, and 60. The data shown are representative results from two independent experiments. *B*, RAG-2$^{-/-}$ mice that have received IL-5Rα$^{-/-}$ B-1 cell transfer show low levels of Igs. On days 30 and 60, the concentrations of Igs in the serum of the recipient mice were determined by isotype-specific ELISA. The mean values of the indicated groups of mice are represented as a bar. **, $p < 0.01$; *, $p < 0.05$; by Student's *t* test.

suggest that IL-5 is also produced by non-T/non-mast/non-eosinophil cells and may support the maintenance and Ab production of mature B-1 cells in vivo.

Defective responses of IL-5Rα$^{-/-}$ B-1 cells to anti-CD40 mAb and LPS

B-1 cells that were smaller in size in IL-5Rα$^{-/-}$ mice and anti-IL-5-treated mice led us to address the possibility that these small cells might show an impaired response to various activation signals. We purified B-1 cells in PECs from IL-5Rα$^{+/+}$ and IL-5Rα$^{-/-}$ mice and stimulated them with anti-CD40, LPS, IL-4, or combinations of these. Interestingly, IL-5Rα$^{-/-}$ B-1 cells showed lower proliferation than did IL-5Rα$^{+/+}$ B-1 cells in response to anti-CD40 (58% of IL-5Rα$^{+/+}$ cells) and LPS (49% of IL-5Rα$^{+/+}$ cells) (Fig. 6*A*). Similar results were obtained when the cells were stimulated with anti-CD40 plus IL-4 and LPS plus IL-4. IL-5Rα$^{-/-}$ B-1 cells secreted significantly lower levels of IgM when they were cultured with anti-CD40, LPS, anti-CD40 plus IL-4, or LPS plus IL-4 than they did IgM secreted from IL-5Rα$^{+/+}$ B-1 cells (Fig. 6*B*, *upper panel*). Although IL-5Rα$^{-/-}$ B-1 cells were capable of producing IgG1 upon stimulation with anti-CD40 plus IL-4 or LPS plus IL-4, the amount of IgG1 produced by these cells was significantly lower (~55% and ~70%, respectively) than the amount of IgG1 produced by IL-5Rα$^{+/+}$ B-1 cells (Fig. 6*B*, *middle panel*). IgG3 production induced by LPS was also impaired in IL-5Rα$^{-/-}$ B-1 cells (Fig. 6*B*, *lower panel*). In contrast with B-1 cells, IL-5Rα$^{+/+}$ and IL-5Rα$^{-/-}$ B-2 cells in the spleen responded comparably upon anti-CD40 or LPS stimulation (data not shown).

Regulation of CD40 expression in B-1 cells by IL-5

One possible reason for the impaired response of IL-5Rα$^{-/-}$ B-1 cells to anti-CD40 may be the impaired expression of CD40. We compared the expression levels of CD40 on IL-5Rα$^{-/-}$ B-1 cells with those on IL-5Rα$^{+/+}$ B-1 cells and found that IL-5Rα$^{-/-}$ B-1 cells showed a significantly lower expression of CD40 than did IL-5Rα$^{+/+}$ B-1 cells (Fig. 7*A*). In contrast with B-1 cells, IL-5Rα$^{-/-}$ B-2 cells showed CD40 expression comparable with that of IL-5Rα$^{+/+}$ B-2 cells. CD40 expression on IL-5$^{-/-}$ B-1 cells was also lower than on wild-type B-1 cells (data not shown). B-1 cells from the anti-IL-5-treated mice showed reduced CD40 expression 6 days after treatment, whereas CD40 expression on B-2 cells was not affected (Fig. 7*B*). Conversely, IL-5 stimulation of IL-5$^{-/-}$ B-1 cells enhanced CD40 expression, whereas CD40 expression on B-2 cells was unaltered (Fig. 7*C*). These results strongly suggest that the IL-5 signal is important for CD40 expression and CD40-related activation in B-1 cells.

Defective IgA production in LPS-administered IL-5Rα$^{-/-}$ mice

As described previously, IL-5Rα$^{-/-}$ B-1 cells respond poorly to LPS stimulation (Fig. 6). Because TLR4/MD2 and RP105 expressed on B cells play an essential role in LPS-mediated B cell activation (43, 44), we examined TLR4/MD2 and RP105 expression on B-1 cells. IL-5Rα$^{+/+}$ B-1 cells showed very low levels of TLR4/MD2 expression and significant levels of RP105 expression. The expression levels of TLR4/MD2 and RP105 on B-1 cells were comparable between IL-5Rα$^{+/+}$ B-1 and IL-5Rα$^{-/-}$ B-1 cells (Fig. 8*A*). IL-5 might not be involved in the regulation of TLR4/MD2 or RP105 expression, but rather might participate in modulating LPS-induced intracellular signaling.

LPS is capable of inducing differentiation of B-1 cells in gut-associated lymphoid tissue (46). We orally administered LPS to IL-5Rα$^{+/+}$ and IL-5Rα$^{-/-}$ mice and examined Ig levels in serum and fecal extracts by ELISA. IgA levels in serum and fecal extracts in LPS-administered IL-5Rα$^{+/+}$ mice were elevated ~40% and ~400%, respectively, compared with those in the PBS-treated control group of mice. The levels of other Ig isotypes were comparable with those in the PBS-treated control mice (Fig. 8*B*). In contrast with the IL-5Rα$^{+/+}$ mice, the IgA levels in serum and fecal extracts in the IL-5Rα$^{-/-}$ mice did not increase as a result of oral LPS administration (Fig. 8*B*). To determine whether impaired IgA production due to LPS administration in IL-5Rα$^{-/-}$ mice was because of a decrease in IgA-producing cells, mononuclear cells were isolated from different tissues in LPS-administered mice and isotype-specific ELISPOT assays were performed. As shown in Fig. 8*C*, we detected a significant number of Ig-producing cells in the LP and PP in both IL-5Rα$^{+/+}$ and IL-5Rα$^{-/-}$ mice. Importantly, the number of IgA-producing cells in the LP and PP was significantly lower in LPS-administered IL-5Rα$^{-/-}$ mice than in LPS-administered IL-5Rα$^{+/+}$ mice. The number of IgM-producing cells in PECs in IL-5Rα$^{-/-}$ mice was also lower than in IL-5Rα$^{+/+}$ mice, whereas their splenocytes showed a number of IgM-producing cells comparable with that in IL-5Rα$^{+/+}$ mice. These results indicate that IL-5 signals are required for cells in the LP and PP to induce the optimal LPS response for terminal differentiation into Ab-producing cells in vivo.

Discussion

IL-5 and B-1 cell maintenance

A significant reduction in B-1 cells has been shown in IL-5Rα$^{-/-}$ and IL-5$^{-/-}$ mice (35, 38) and in 129 mice whose B cells show impaired response to IL-5 (47). These results imply that IL-5 is a

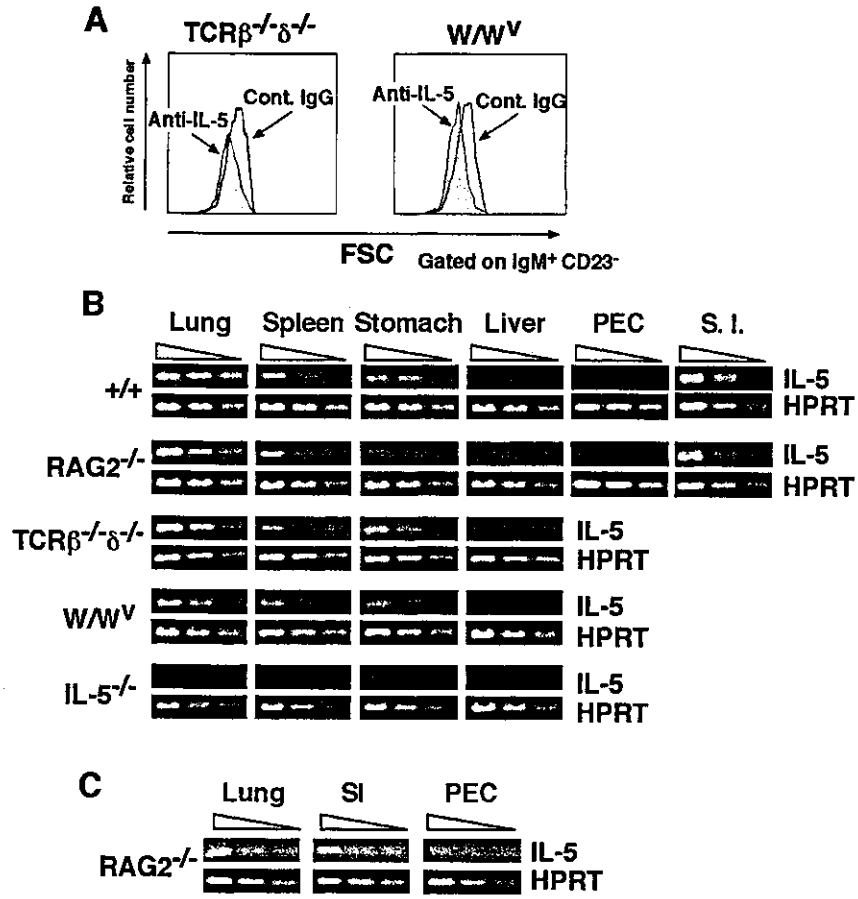

FIGURE 5. IL-5 production by cells other than T cells, mast cells, and eosinophils. *A*, Anti-IL-5 Ab treatment affects B-1 cell maintenance in T cell- or mast cell-deficient mice. A single i.p. administration of anti-IL-5 mAbs or control IgG (1 mg/250 μl) into TCR$\beta^{-/-}\delta^{-/-}$ or W/W^{V} mice was performed. On day 6 after treatment, peritoneal cells were obtained and analyzed. Representative histograms depict the relative cell number and size of the B-1 cells. Representative results of three independent experiments are shown. *B*, Tissues from T cell- or mast cell-deficient mice show *IL-5* mRNA expression. Various tissues were freshly isolated from IL-5R$\alpha^{+/+}$, RAG-2$^{-/-}$, TCR$\beta^{-/-}\delta^{-/-}$, W/W^{V}, and IL-5$^{-/-}$ mice. *C*, Non-T/non-mast/non-eosinophil cells express *IL-5* mRNA. Single cell suspensions were prepared from the lungs, small intestine (SI), and PECs of RAG-2$^{-/-}$ mice and c-*kit*$^{-}$ and IL-5Rα^{-} cells purified by negative sorting using MACS (>99% purity). Serial dilutions (4-fold) of cDNA templates were prepared and subjected to RT-PCR analysis using primer sets designed to amplify *IL-5* or HPRT cDNA fragments (*B* and *C*).

crucial cytokine for B-1 cell development or maintenance. Supporting this notion, we showed B-1 cells that were fully restored in number and function in IL-5R$\alpha^{-/-}$ mice due to the enforced expression of IL-5Rα by crossing with IL-5Rα transgenic mice (36). It should be noted that the decrease in B-1 cell proportion and number is more obvious in young IL-5R$\alpha^{-/-}$ mice than in older ones. This suggests that the IL-5 signal is at least required to facilitate B-1 cell development. However, it is not clear whether IL-5 is required for the maintenance of mature B-1 cells. Thus, the key question is to what extent IL-5 is involved in mature B-1 cell survival and homeostatic proliferation.

This study demonstrates the marked impairment of the maintenance of mature B-1 cell survival and its homeostatic proliferation by blocking IL-5 signals. Intriguingly, the administration of anti-IL-5 mAb into IL-5R$\alpha^{+/+}$ mice could induce a rapid reduction in the total number and size of B-1 cells within 6 days to a degree comparable with that observed in IL-5R$\alpha^{-/-}$ B-1 cells (Fig. 1*B*). Cell transfer experiments of CFSE-labeled B-1 cells to wild-type mice revealed that CFSE^{+} B-1 cells from wild-type mice survived longer in the peritoneal cavity than did those from IL-5R$\alpha^{-/-}$ B-1 cells (Fig. 2). This may not be due to the impairment of the migratory activity of IL-5R$\alpha^{-/-}$ B-1 cells, because the distribution pattern of CFSE-positive IL-5R$\alpha^{-/-}$ B cells in the LP, PP, and MLNs in the recipient mice 30 days after cell transfer was similar to that of CFSE-positive IL-5R$\alpha^{+/+}$ B cells (data not shown). We were surprised to see CFSE-positive B-2 cells (>50% more than starting cells) in the recipients 30 days after cell transfer, because B-2 cells are thought to be recirculating cells that do not reside in the peritoneal cavity. A proportion of B-2 cells in the peritoneal cavity tend to reside in or to migrate to the peritoneal cavity.

CFSE-labeled B-1 cells of wild-type mice expanded in the peritoneal cavity on day 30 of cell transfer in the RAG-2$^{-/-}$ mice, whereas IL-5R$\alpha^{-/-}$ B-1 cells did not (Figs. 3, *A* and *B*, and 4*A*). This again may not be due to the enhanced migration of IL-5R$\alpha^{-/-}$ B-1 cells in RAG-2$^{-/-}$ mice to the B cell compartment other than in the peritoneal cavity, because IL-5R$\alpha^{-/-}$sIgA^{+} B cells resided in the LP to lesser extent than did IL-5R$\alpha^{+/+}$sIgA^{+} B cells (Fig. 3*C*). The CFSE-labeled B-2 cells in RAG-2$^{-/-}$ mice expressed a wide range of CFSE labeling intensities (Fig. 3*B*). It is likely that cotransferred T cells may expand in the peritoneal cavity of RAG-2$^{-/-}$ recipient mice because of their ability to homeostatically proliferate, during which they may produce cytokines that induce the proliferation of B-2 cells. Alternatively, the B-2 cells that we detected may have been contaminated B-1 cell progenitors with long-lived and self-replenishing activity.

We were surprised to observe that both IL-5R$\alpha^{+/+}$sIgA^{+} B cells and IL-5R$\alpha^{-/-}$sIgA^{+} B cells showed relatively low CFSE labeling (Fig. 3*C*), suggesting extensive cell divisions before differentiation to sIgA^{+} B cells. Although CFSE intensities of B cells were similar, a reduced proportion of sIgA^{+} B cells in the LP of RAG-2$^{-/-}$ mice transferred with IL-5R$\alpha^{-/-}$ B cells was observed compared with mice transferred with IL-5R$\alpha^{+/+}$ B cells. This may be due to the impairment of cell survival and expansion of IL-5R$\alpha^{-/-}$ B-1 cells, although a small proportion of IL-5R$\alpha^{-/-}$ B-1 cells may be sufficient for proliferation and differentiation to sIgA^{+} B cells. Our results imply that the IL-5/IL-5R system plays an important role in maintaining mature B-1 cell survival and homeostatic proliferation in our short-term cell transfer assay.

IL-5-dependent B-1 cell maintenance in T cell- and mast cell-deficient mice

Although it is well known that T cells are a major IL-5 producer, we observed IL-5-mediated homeostatic proliferation of purified B-1 cells in recipient RAG-2$^{-/-}$ mice (Fig. 4). It was possible that

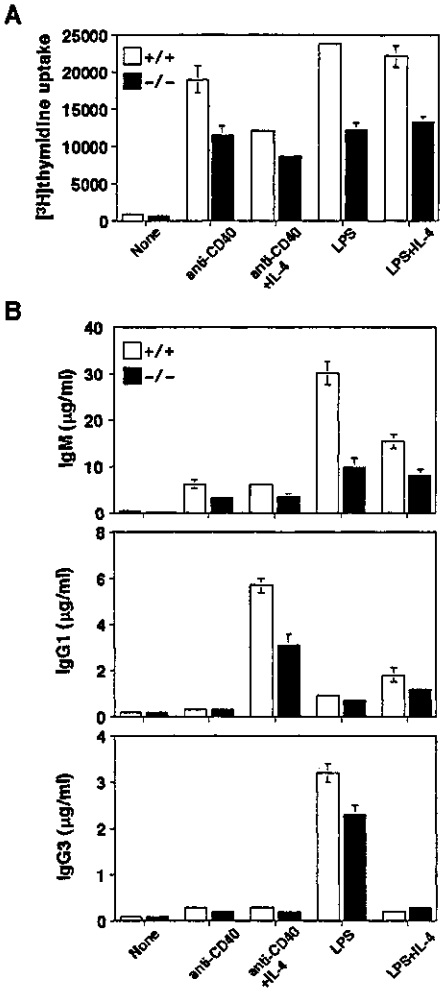

FIGURE 6. Defective activation of IL-5R$\alpha^{-/-}$ B-1 cells to anti-CD40 mAb or LPS. *A*, IL-5R$\alpha^{-/-}$ B-1 cells have defective proliferative responses to anti-CD40 mAb or LPS. B-1 cells purified by the MACS system were cultured (1×10^5 cells in a 200-μl culture) for 3 days with anti-CD40 mAb (1 μg/ml), LPS (40 μg/ml), IL-4 (1000 U/ml), or a selected combination of these agents. The cells were pulse-labeled with [^{3}H]thymidine (0.2 μCi/well) for the last 8 h of the culture. The results represent the mean cpm ± SD of the duplicate determinations. *B*, IL-5R$\alpha^{-/-}$ B-1 cells produce a small amount of Igs in response to anti-CD40 mAb or LPS. Purified B-1 cells were cultured (1×10^5 cells in a 200-μl culture) for 7 days with each stimulant as described in *A*. The IgM, IgG1, and IgG3 concentrations in the cultured supernatants were determined by ELISA. The values represent the mean and SD of the duplicate wells. The data shown are representative results from three independent experiments (*A* and *B*).

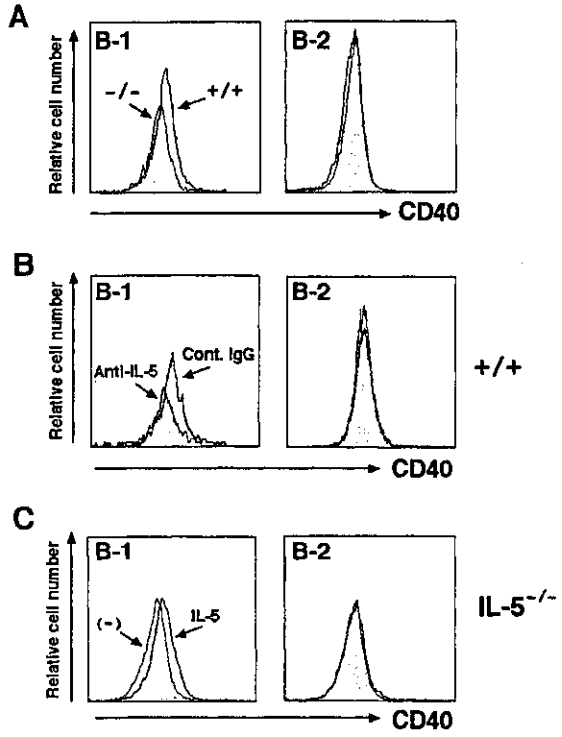

FIGURE 7. IL-5-dependent CD40 expression on B-1 cells. *A*, IL-5R$\alpha^{-/-}$ B-1 cells express low levels of CD40. *B*, Decreased CD40 expression on B-1 cells from anti-IL-5-treated mice is reduced. *C*, CD40 expression on IL-5$^{-/-}$ B-1 cells is recovered by IL-5 stimulation. Peritoneal cells from IL-5$^{-/-}$ mice were cultured (1×10^6 cells in a 2-ml culture) for 2 days with or without IL-5 (500 U/ml). The cultured cells were stained and analyzed by flow cytometry. Representative histograms show the CD40 expression of B-1 or B-2 cells from IL-5$^{-/-}$ mice, which were cultured for 2 days. Representative results from three different experimental sets are shown.

extremely low numbers of T cells in RAG-2$^{-/-}$ mice may provide T cell help, as described by Kushnir et al. (48), but we found no significant T cell population when we examined the PECs from RAG-2$^{-/-}$ mice 30 days after purified B-1 cell transfer (data not shown). Moreover, the results in which anti-IL-5-treated T cell-deficient mice show a reduction in number and cell size of B-1 cells in the peritoneal cavity also support our conclusion that non-T cells produce the IL-5 that supports maintenance and Ab production by B-1 cells (Fig. 5*A*). In fact, cells in various tissues including the lungs, stomach, and spleen of RAG-2$^{-/-}$ mice or TCR$\beta^{-/-}\delta^{-/-}$ mice showed *IL-5* mRNA expression (Fig. 5*B*). Moreover, small intestine and peritoneal washouts also expressed *IL-5* mRNA. Fort et al. (49) demonstrated using RAG-2$^{-/-}$ splenocytes that non-T/non-B cells produce IL-5 in response to IL-25 and that cells responding to IL-25 are accessory cells, which belong to the MHC class II^{high}, CD11c^{dull}, F4/80^{low}, CD8α^-, and CD4$^-$ populations. In vitro stimulation of mouse mast cells by FcϵRI cross-linking induces increased levels of mRNA expression or secretion of various inflammatory cytokines including IL-5 (50). W/W^V mice showed *IL-5* mRNA expression and IL-5-dependent B-1 cell maintenance (Fig. 5, *A* and *B*). In addition to T cells and mast cells, eosinophils and NK cells have also been shown to possess IL-5-producing ability (51, 52). This study shows that c-*kit*$^-$IL-5Rα^- cells purified from the lungs and small intestine of RAG-2$^{-/-}$ mice expressed *IL-5* mRNA (Fig. 5*C*). Our results support the notion that IL-5 can be produced even in T cell-, mast cell-, and eosinophil-deficient conditions, possibly by nonhemopoietic cells, leading to the support of B-1 cell maintenance.

IL-5 and CD40-related response of B-1 cells

T cell-dependent activation of B cells requires CD40-CD40 ligand (CD40L) interaction and a defined set of cytokines. Although B-1 cells are classified as B cells responding to T cell-independent Ags, T cells can influence other aspects of B-1 cell activation and differentiation. In fact, B-1 cells exhibit a strong proliferation and IgG1 production when cocultured with activated T cells plus IL-4 or with recombinant CD40L plus IL-4 (53). T cells enhance Ig production by B-1 cells and induce switching from IgM to IgG1 in B-1 cell-transferred SCID mice (10). Moreover, Erickson et al. (53) have demonstrated that B-1 cells require IL-5 in conjunction with CD40-CD40L interaction for maximal T cell-dependent responses. We showed that IL-5 regulates CD40 expression solely